Electronic Supplementary Material (ESI) for Chemical Communications.

Charge "Mis-matched" Hydrogen Bonded Frameworks for Cation Exchange and Dye Sorption

Phonlakrit Muang-Non,[a] Adrian W. Markwell-Heys,[b] Christian J. Doonan[b] and Nicholas G. White[a]*

[a] *Research School of Chemistry, The Australian National University, 137 Sullivan's Creek Road, Acton, 2600, ACT, Australia. Email: nicholas.white@anu.edu.au URL: www.nwhitegroup.com.*

[b] *Department of Chemistry and the Centre for Advanced Nanomaterials, The University of Adelaide, Adelaide, South Australia, 5005, Australia.*

Synthesis and Characterisation **2**

Detail of instrumentation 2

Synthesis of organic building blocks 2

Synthesis of hydrogen bonded frameworks 4

Cation exchange of TBA·2_2·B **13**

Cation exchange crystallisations 13

^{1}H NMR experiments 14

X-ray crystallography **16**

General remarks 16

Summary of crystallographic data 17

Details of individual refinements 18

Methylene blue and crystal violet adsorption **28**

UV Vis spectroscopy (28 μM, 1.0 equivalent framework) 29

UV Vis spectroscopy (55 μM, 1.0 equivalent framework) 31

UV Vis spectroscopy (1.5 and 2.0 equivalents framework) 32

Photographs 33

^{1}H NMR spectroscopy 34

References **35**

Synthesis and Characterisation

Details of instrumentation

NMR spectra were collected on Bruker Avance 400 and are referenced to the residual solvent signal.[1] Infrared spectra were recorded on a Perkin-Elmer Spectrum Two FT-IR Spectrometer fitted with an ATR Two Single Reflection Diamond. UV-Vis spectra were collected on a Perkin-Elmer Lambda 465 spectrometer. Electrospray ionisation mass spectrometry data were acquired on a Micromass Waters ZMD spectrometer. PXRD data were collected using a PANalytical diffractometer with Cu K_α radiation and a PIXcel detector. TGA data were recorded on a TA Instruments Q500 analyser under flowing nitrogen at a ramp speed of 5 °C/minute.

Synthesis of organic building blocks

The tetraamidinium **1·Cl$_4$**[2] and biphenylbisamidinium **2·Cl$_2$**[3] were synthesized as previously described. The new tetrabutylammonium (TBA) salt of borate-tetracarboxylate, *i.e.* **TBA$_5$·B**, was prepared from ammonium borate-tetracarboxylic acid (**NH$_4$·B^{4H}**)[4] as shown in Scheme 1. Other chemicals, including the chloride salts of MB^+ and CV^+ were bought from commercial suppliers and used as received.

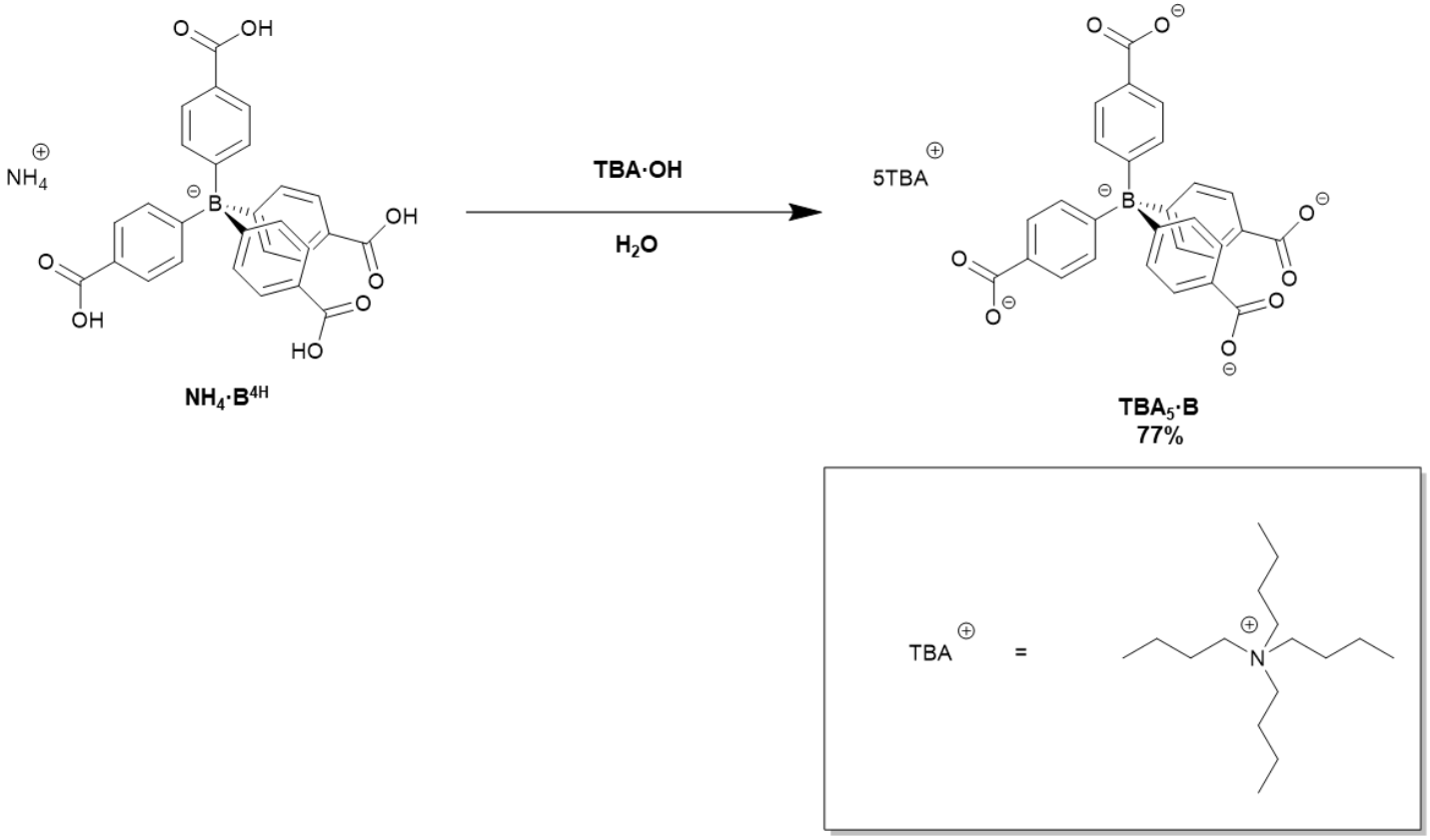

NH$_4$·B^{4H} **TBA$_5$·B** **77%**

Scheme S1. Synthesis of **TBA$_5$·B**.

Synthesis of TBA_5·B

The ammonium salt of the tetracarboxylic acid, *i.e.* **NH_4·B^{4H}**,[4] (0.51 g, 1.0 mmol) was suspended in water (5 mL). Tetrabutylammonium hydroxide in methanol (1.0 M, 6.0 mL, 6.0 mmol) was added to the reaction mixture and stirred for 10 minutes, which caused the suspension to dissolve. The reaction mixture was taken to dryness under reduced pressure giving a brown powder. Excess tetrabutylammonium hydroxide was removed by dissolving the crude material in hot acetone (6 mL) and precipitating using diethyl ether (20 mL). The resulting white powder was isolated by filtration, washed with diethyl ether (2 × 10 mL) and air-dried.

Yield: 1.13 g (77%).

^{1}H NMR (400 MHz, d_6-DMSO): 7.41 (d, *J* = 7.5 Hz, 8H), 7.03–7.07 (m, 8H), 3.19–3.28 (m, 40H), 1.56–1.64 (m, 40H), 1.30–1.39 (m, 40H), 0.97 (t, *J* = 7.4 Hz, 60H) ppm.

^{13}C NMR (400 MHz, d_6-DMSO): 170.9, 164.2–165.7 (m), 135.8, 134.8, 126.5, 58.0, 23.6, 19.7, 14.0 ppm.

ESI-MS (neg.): 491.3, calc. for $[C_{28}H_{16}BO_4]^{5-}$, *i.e.* $[\mathbf{B}]^{5-}$ = 491.2 Da.

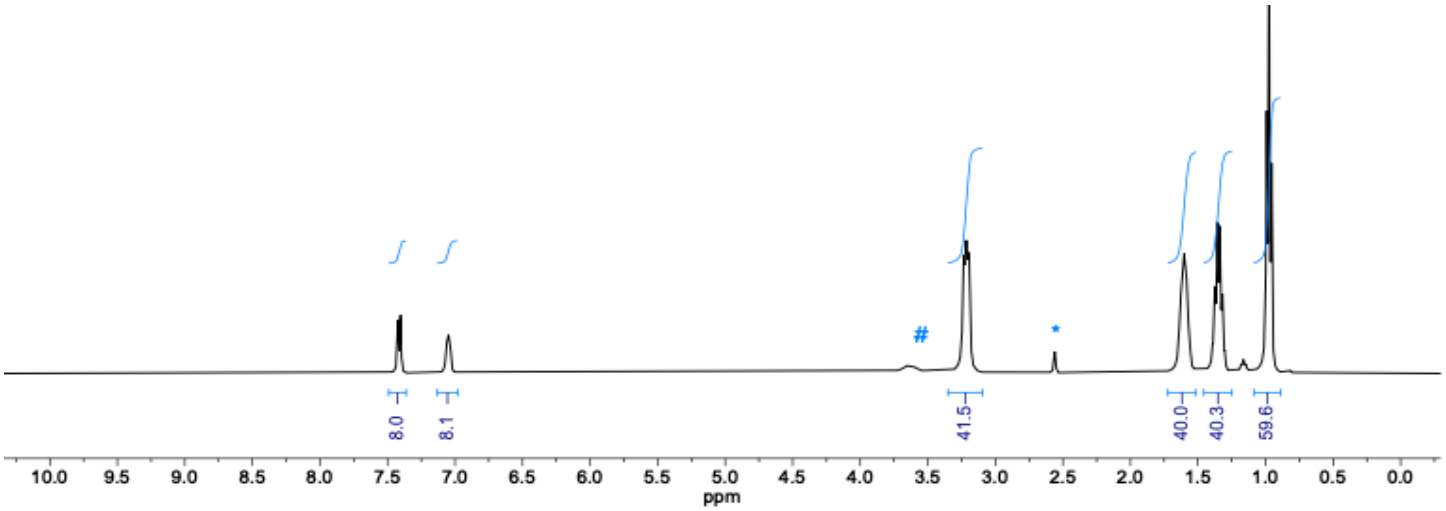

Figure S1. ^{1}H NMR spectrum of **TBA_5·B**, peak labelled * results from incompletely deuterated NMR solvent, peak labelled # results from water (d_6-DMSO, 400 MHz, 298 K).

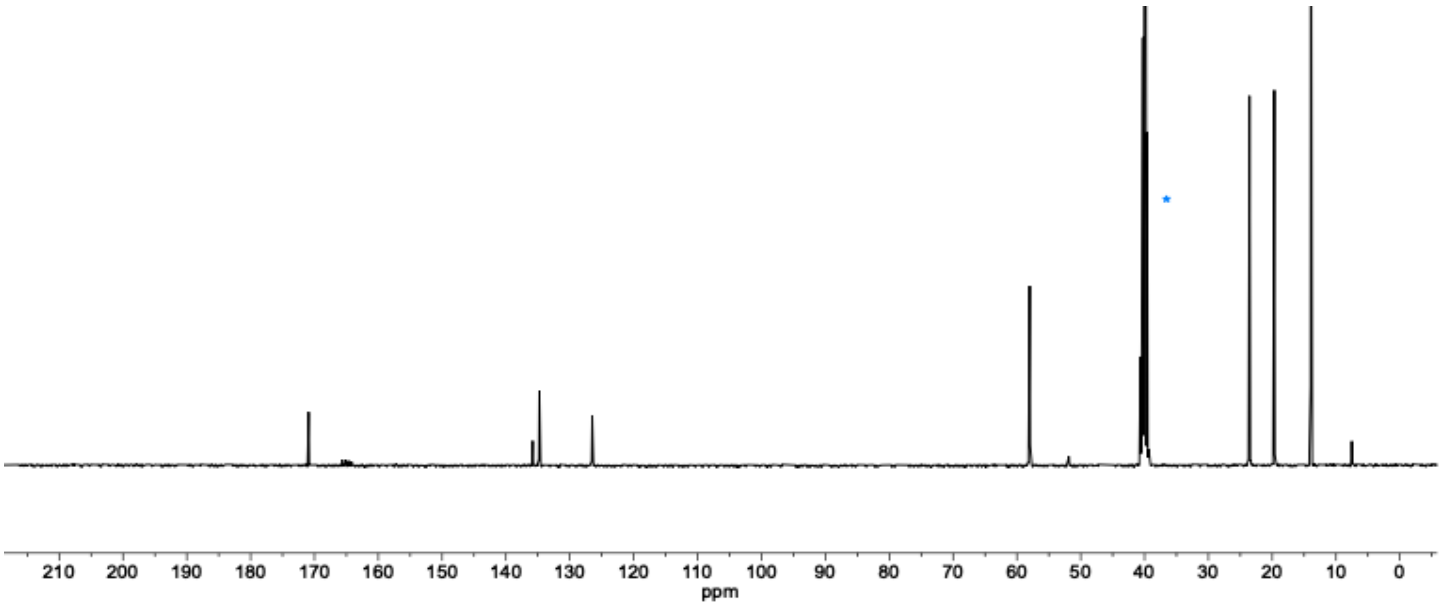

Figure S2. ^{13}C NMR spectrum of **TBA_5·B**, peak labelled * results from incompletely deuterated NMR solvent (d_6-DMSO, 400 MHz, 298 K).

Synthesis of hydrogen bonded frameworks

After several days, all frameworks were isolated by filtration, washed with small amount of water, and then dried using mild vacuum. The frameworks were suspended in d_6-DMSO and digested using a drop of concentrated $HCl_{(aq)}$ for NMR analysis. Thermogravimetric analysis (TGA) and powder X-ray diffraction (PXRD) traces of all frameworks were recorded on material that had been dried under mild vacuum; all framework yields account for the presence of solvents indicated by TGA.

Crystallization conditions

Initially, we crystallized the frameworks from either water or a H_2O:EtOH mixture using a borate:amidinium molar ratio of 1:1 and 1:2 ratio for **1·Cl₄** and **2·Cl₂**, respectively, which resulted in single crystals. Using the "correct" ratio (ignoring additional cations), *i.e.* a 4:5 and 2:5 ratio for **1·Cl₄** and **2·Cl₂**, respectively, gave identical unit cells in both cases. The outcome of all borate frameworks varied depending on the crystallization conditions. A summary of these conditions is provided in Table S1.

Table S1. Summary of crystallisation conditions and outcomes for amidinium-borate systems.

Components used (cation·anion)	Solvent[a]	Additive	Conc. cation (mM)	Outcome[b]	Framework
1·B	H_2O		0.50 – 2.0	✓	**TBA·1·B**
			0.25	✗	
	H_2O	100 equiv. NaCl	2.0	✓	**TBA·1·B**
		100 equiv. NaI	2.0	✓	**TBA·1·B**
		100 equiv. KI	2.0	✓	**TBA·1·B**
	0 – 10% EtOH		2.0	✗	
	20-80% EtOH		2.0	✓	**"1·B"** [c]
	90% EtOH		2.0	✗	
	EtOH		2.0	✗	
	50% EtOH	100 equiv. NaCl	2.0	✓	**"1·B"** [c]
		100 equiv. NaI	2.0	✓	**"1·B"** [c]
		100 equiv. KI	2.0	✓	**"1·B"** [c]
2·B	H_2O		2.0	✗	
			0.50 – 1.0	✓	**$2_{2.5}$·B**
			0.25	✗	
	50% EtOH		1.0 – 2.0	✓	**TBA·2_2·B**
			0.25 – 0.50	✗	
	H_2O	100 equiv. NaCl	1.0	✗	
		100 equiv. NaI	1.0	✗	
		100 equiv. KI	1.0	✗	
	50% EtOH	100 equiv. NaCl	1.0	✓	**Na·2_2·B**
		100 equiv. NaI	1.0	✗	
		100 equiv. KI	1.0	✗	

[a] Volume % EtOH in water. [b] A cross indicates non-crystalline products were obtained, a tick indicates well-formed crystals were obtained. [c] These conditions resulted in low quality single crystals, but we could not identify the product definitively due to the poor quality of the data.

Synthesis of TBA·1·B

TBA_5·B (14.1 mg, 8.28 µmol) was dissolved in water (2 mL) and added to a solution of **1·Cl_4** (5.01 mg, 7.90 µmol) in water (2 mL), and the resulting cloudy solution left to stand at room temperature. The cloudiness disappeared and needle crystals were observed after approximately 24 hours. After two days, the clear needle crystals were isolated by filtration, washed with water (3 mL) and air-dried**.**

Yield: 5.32 mg (4.10 µmol, 53%).

^{1}H NMR (400 MHz, d_6-DMSO containing a drop of conc. $HCl_{(aq)}$): 9.64 (br. s, 8H), 9.39 (br. s, 8H), 8.01 (d, *J* = 8.7 Hz, 8H), 7.60–7.65 (m, 16H), 7.28–7.30 (m, 8H), 3.19–3.22 (m, 8H), 1.54–1.67 (m, 8H), 1.27–1.41 (m, 8H), 0.90–1.00 (m, 12H) ppm.

ATR-IR (*inter alia*): 1017 (B-C stretching) cm^{-1}.

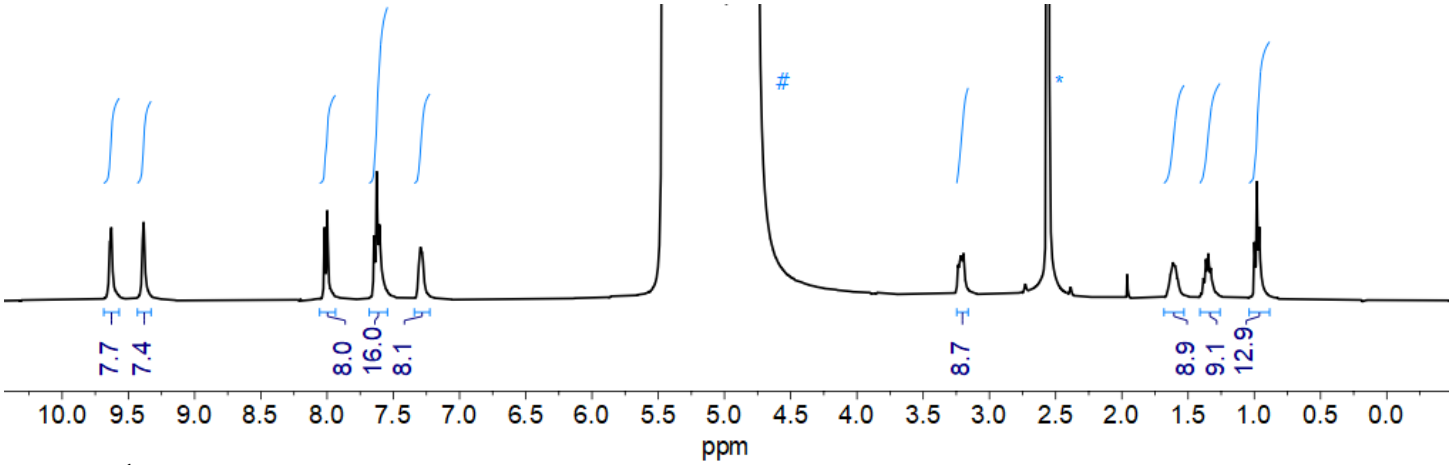

Figure S3. ^{1}H NMR spectrum of acid-digested **TBA·1·B**; peak labelled * results from incompletely deuterated NMR solvent, peak labelled # results from water (d_6-DMSO containing 1 drop $HCl_{(aq)}$, 400 MHz, 298 K).

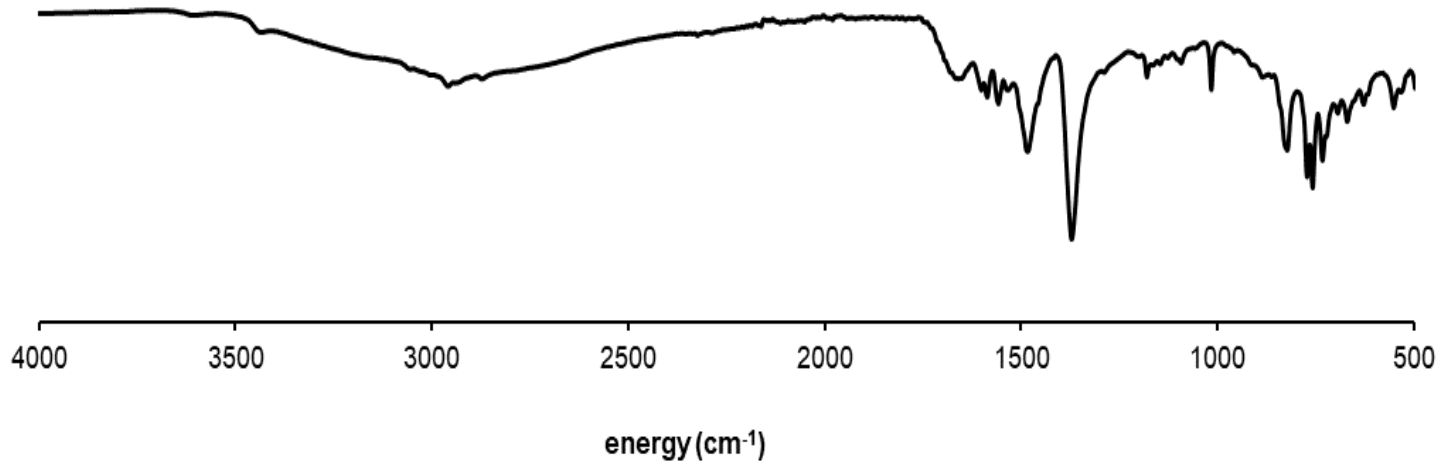

Figure S4. ATR-IR spectrum of **TBA·1·B**.

Upon heating **TBA·1·B** lost 4.2% mass which corresponds to that expected for 3 water molecules (Figure S5).

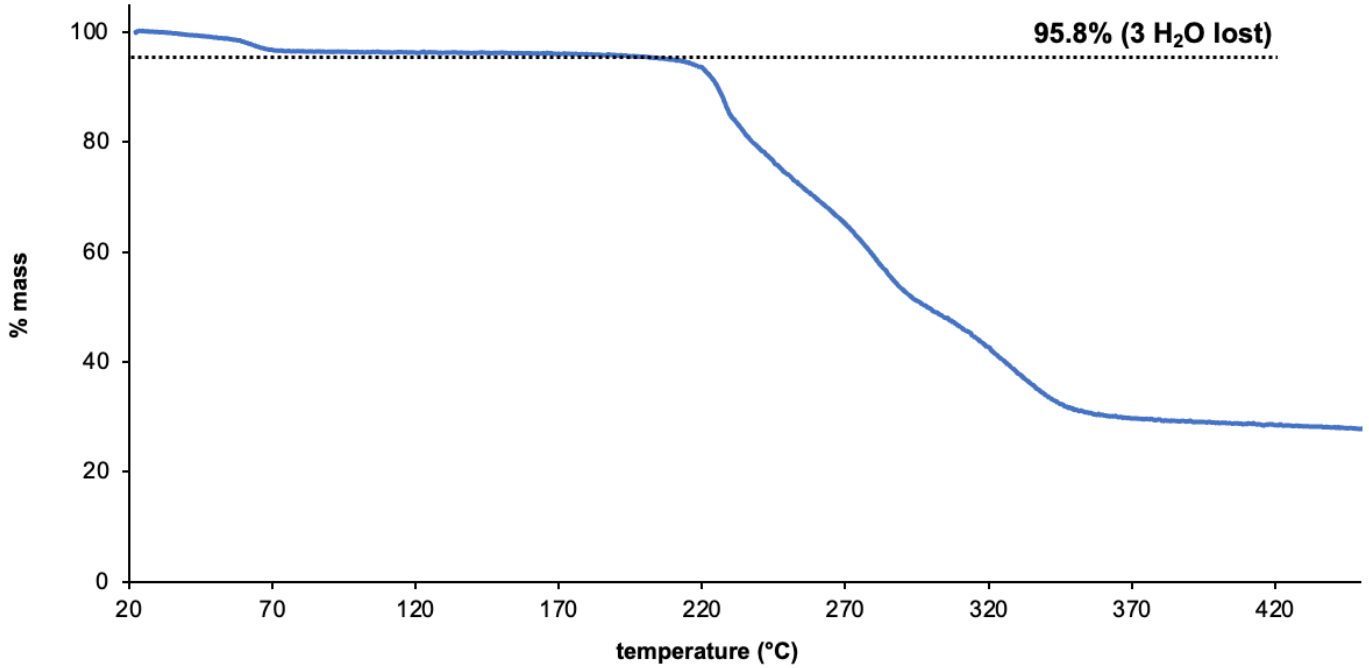

Figure S5. TGA trace of **TBA·1·B**. The black dotted line indicates the expected mass lost corresponding to water solvents from framework.

TBA·1·B retained crystallinity after drying using mild vacuum as shown by powder X-ray diffraction (Figure S6). However, the pattern was different to the pattern calculated from the SCXRD structure, which may be due to the rearrangement of the framework upon drying. The crystal structure of **TBA·1·B** contains large solvent-filled voids while TGA of the dried material shows only a small mass loss, suggesting that significant water is lost upon drying, presumably causing the structural rearrangement observed by PXRD. Measuring the PXRD on freshly-isolated (*i.e.* not dried) material gave a different trace from the dried sample, but this still did not match well with that expected based on the SCXRD data.

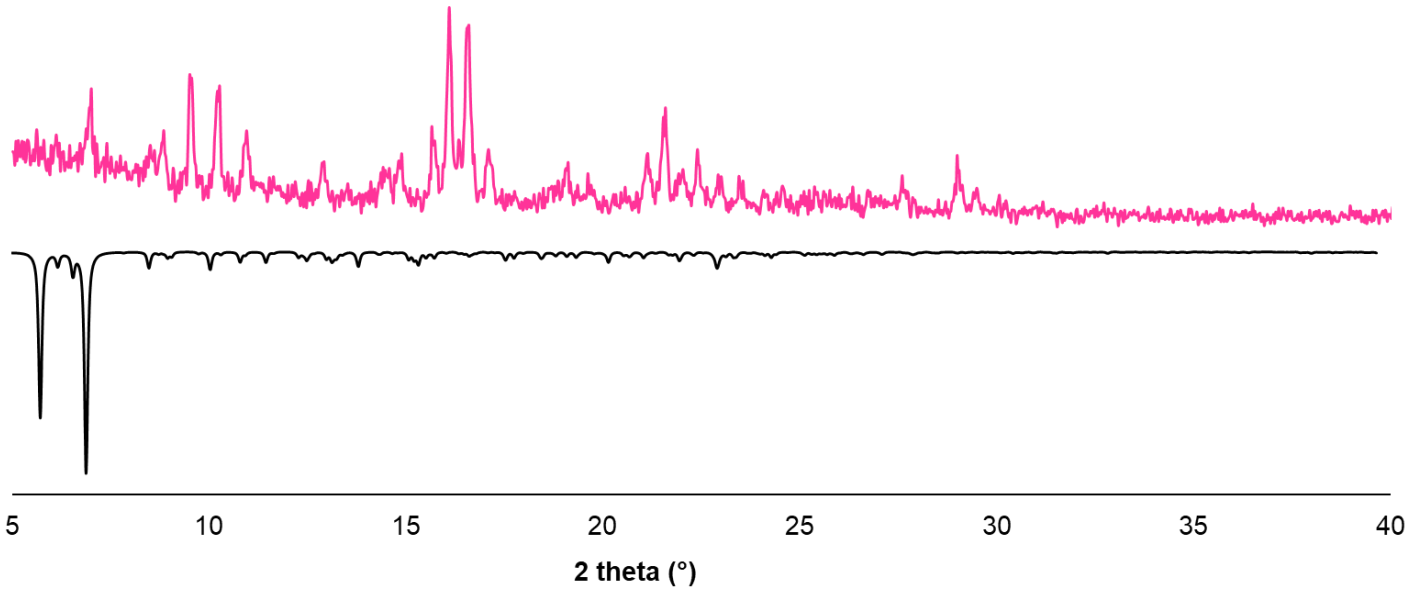

Figure S6. PXRD pattern of **TBA·1·B** sample (red) and the respective calculated trace (black) from crystallography data.

Synthesis of $\mathbf{2}_{2.5}$·**B**

TBA_5·B (34.1 mg, 20.0 µmol) was dissolved in H_2O (10 mL) and added to a solution of **2·Cl_2** (12.2 mg, 39.2 µmol) in H_2O (10 mL), and the cloudy solution left to stand at room temperature. Crystals were observed after approximately 1 hr. After two days, the clear needle crystals were isolated by filtration, washed with water (10 mL) and air-dried.

Yield: 15.9 mg (13.3 µmol, 85%).

^{1}H NMR (400 MHz, d_6-DMSO containing a drop of conc. $HCl_{(aq)}$): 9.63 (br. s, 8H), 9.32 (br. s, 8H), 8.01 (s, 20H), 7.59 (d, *J* = 8.1 Hz, 8H),7.18–7.22 (m, 8H) ppm.

ATR-IR (*inter alia*): 1010 (B–C stretching) cm^{-1}.

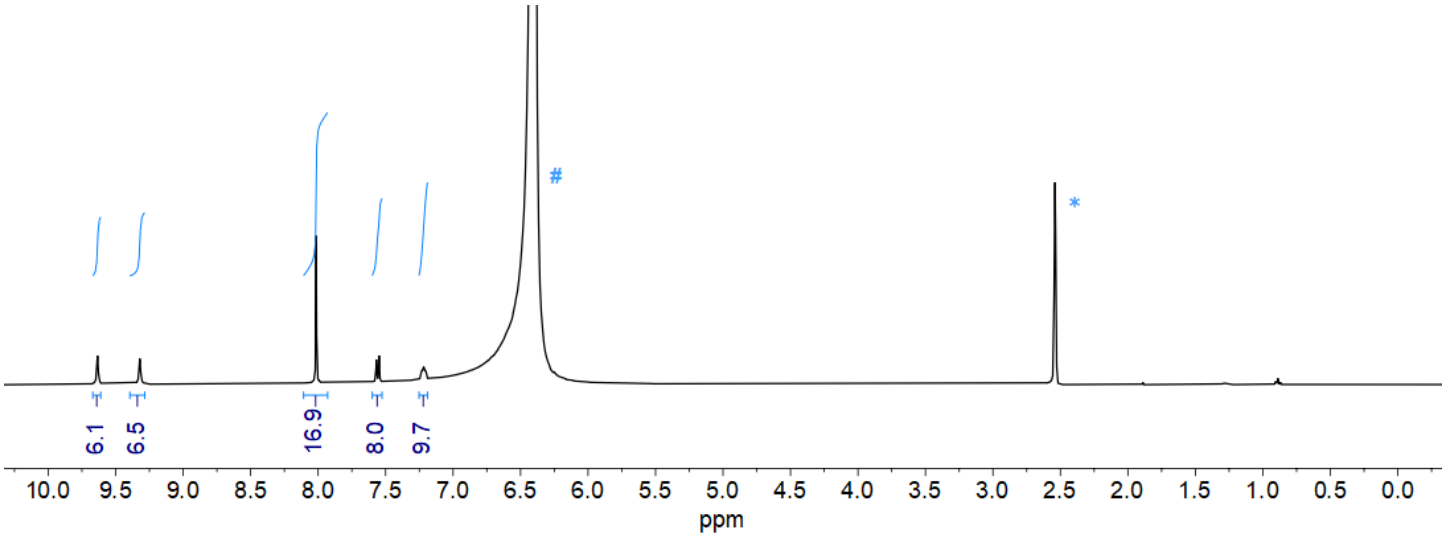

Figure S7. ^{1}H NMR spectrum of **$2_{2.5}$·B**; peak labelled * results from incompletely deuterated NMR solvent, peak labelled # results from water (d_6-DMSO containing 1 drop $HCl_{(aq)}$, 400 MHz, 298 K).

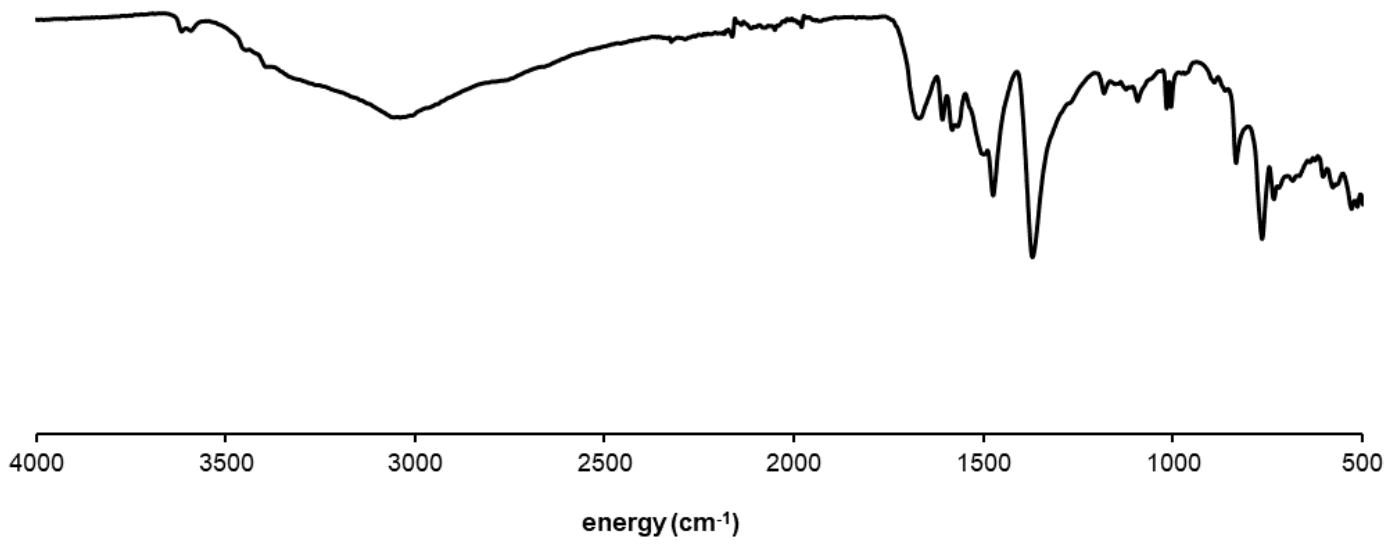

Figure S8. ATR-IR spectrum of **$2_{2.5}$·B**.

Upon heating **$2_{2.5}$·B** lost 9.0% mass which corresponds to that expected for 6 water molecules (Figure S9).

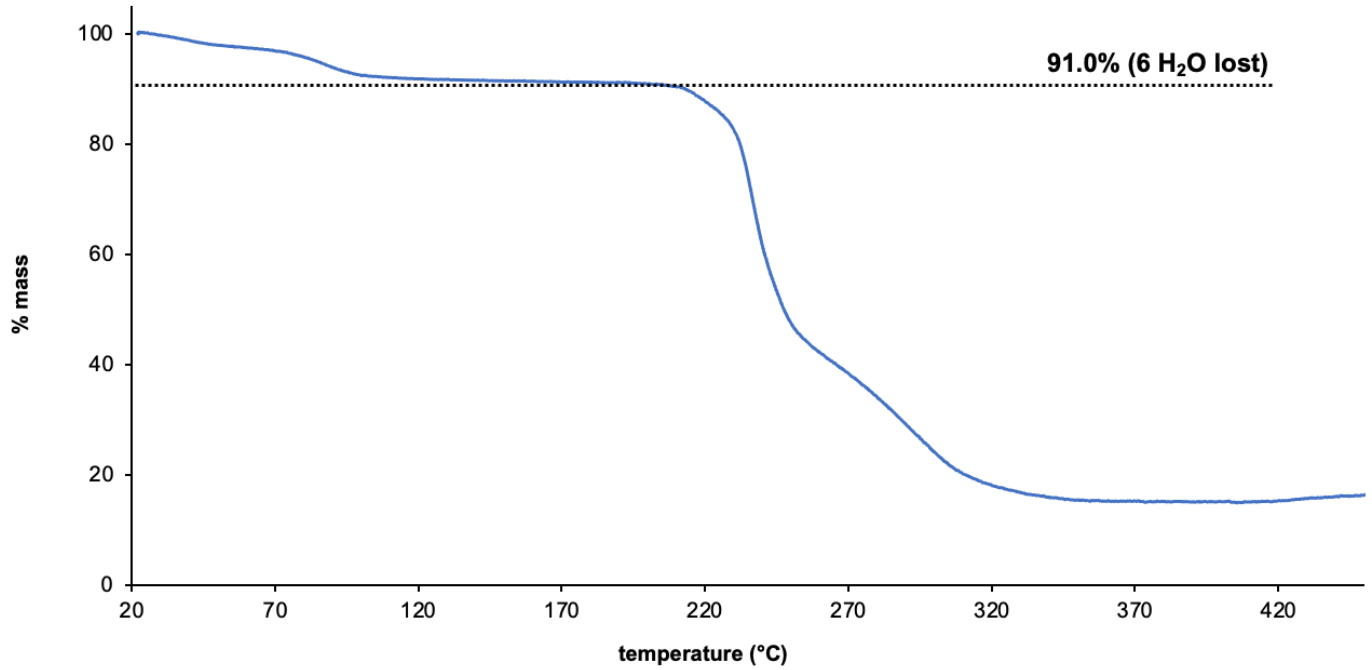

Figure S9. TGA trace of **$2_{2.5}$·B**. The black dotted line indicates the expected mass lost corresponding to water solvents from framework.

$2_{2.5}$·B retains its crystallinity upon drying (Figure S10), which may be due to its relatively dense structure. The PXRD data are a relatively good match for those calculated from the SCXRD structure.

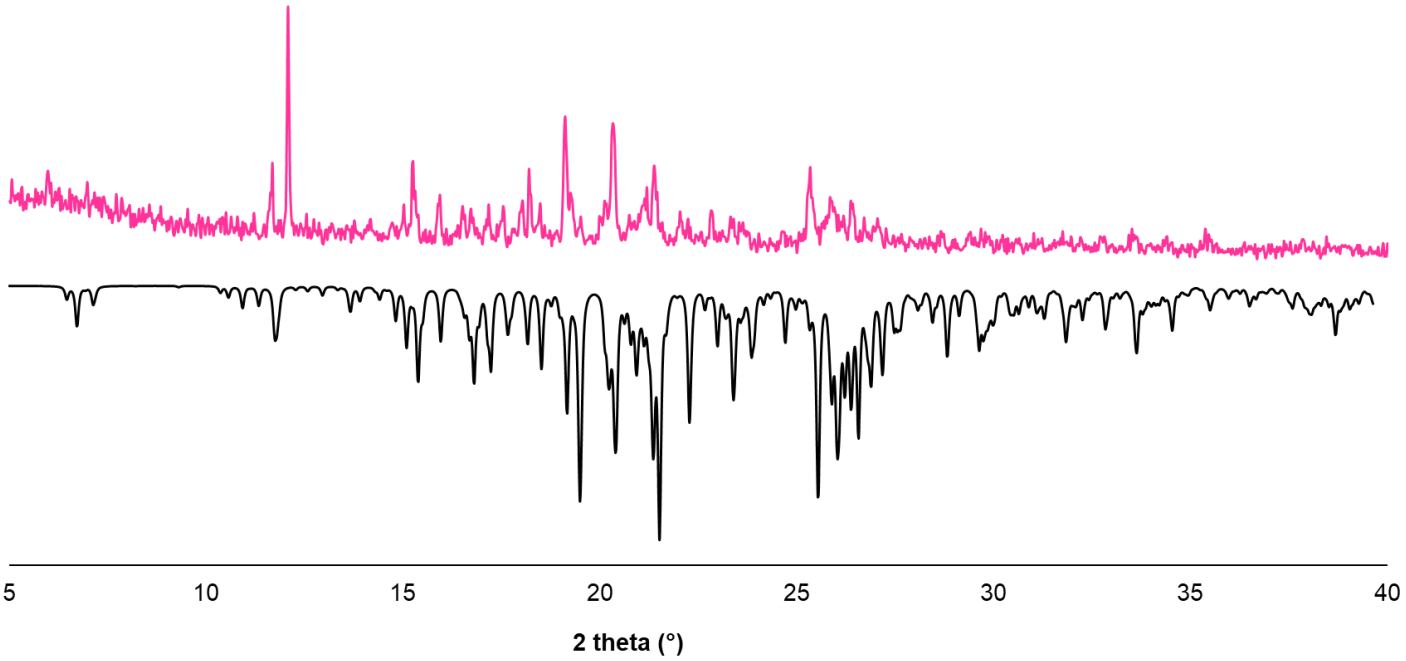

Figure S10. PXRD pattern of **$2_{2.5}$·B** sample (red) and the trace calculated from SCXRD data (black).

Synthesis of TBA·2_2·B

TBA_5·B (68.2 mg, 40.0 µmol) was dissolved in 1:1 EtOH:H_2O (20 mL) and added to a solution of **2·Cl_2** (25.1 mg, 80.7 µmol) in 1:1 EtOH:H_2O (20 mL), and the cloudy solution left to stand at room temperature. Within 5 hours the cloudiness had cleared and needle crystals were observed. After two days, the clear needle crystals were isolated by filtration, washed with water (10 mL) and air-dried.

Yield: 35.1 mg (26.2 µmol, 65%).

^{1}H NMR (400 MHz, d_6-DMSO containing a drop of conc. $HCl_{(aq)}$): 9.65 (br. s, 8H), 9.40 (br. s, 8H), 8.05 (s, 16H), 7.59 (d, *J* = 8.1 Hz, 8H), 7.21–7.30 (m, 8H), 3.12–3.24 (m, 8H), 1.51–1.64 (m, 8H), 1.25–1.37 (m, 8H), 0.93 (t, *J* = 7.3 Hz, 12H) ppm.

ATR-IR (*inter alia*): 1006 (B-C stretching) cm^{-1}.

TBA·2_2·B loses crystallinity upon drying. When we collected the PXRD of the framework before drying, we obtained a PXRD trace containing some very weak peaks, however these did not appear to match well with those expected based on the SCXRD structure of **TBA·2_2·B**. Leaving the material exposed to the air for a few minutes caused these peaks to disappear, consistent with the material rapidly losing crystallinity.

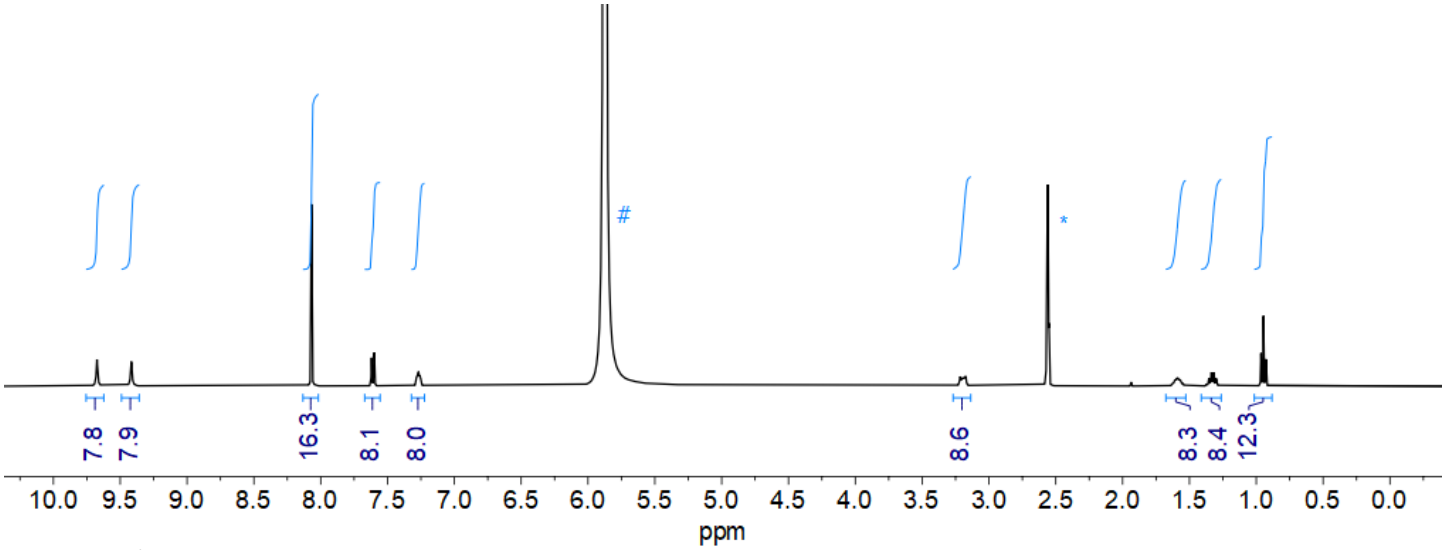

Figure S11. ^{1}H NMR spectrum of acid-digested **TBA·2_2·B** peak labelled * results from incompletely deuterated NMR solvent, peak labelled # results from water (d_6-DMSO containing 1 drop $HCl_{(aq)}$, 400 MHz, 298 K).

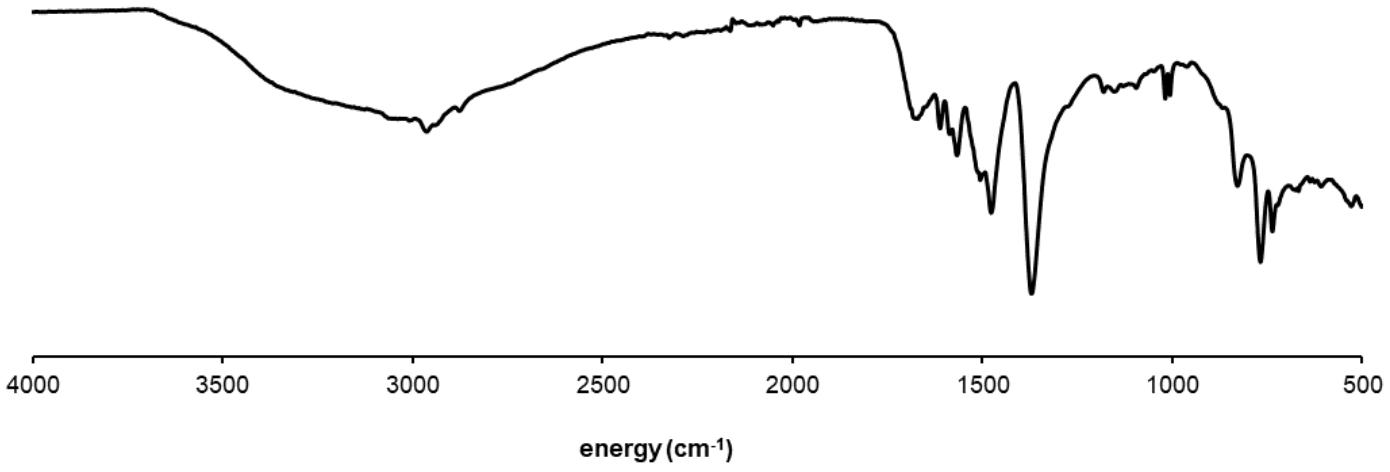

Figure S12. ATR-IR spectrum of **TBA·2_2·B**.

Upon heating **TBA·2$_2$·B** lost 9.4% mass which corresponds to that expected for 7 water molecules (Figure S13).

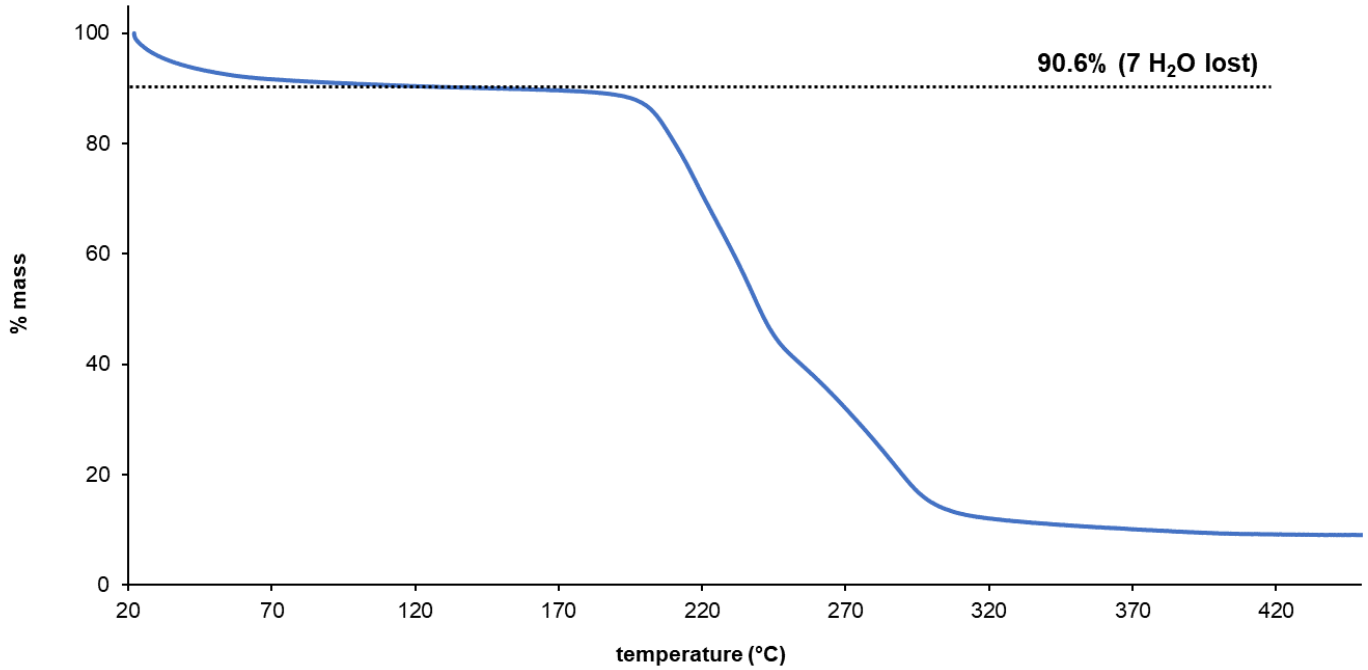

Figure S13. TGA trace of **TBA·2$_2$·B**. The black dotted line indicates the expected mass lost corresponding to water solvents from framework.

Synthesis of Na·2₂·B

TBA_5·B (34.2 mg, 20.1 µmol) was dissolved in 1:1 H_2O:EtOH (5 mL) and added to a solution of NaCl (229 mg, 3.92 mmol) in 1:1 H_2O:EtOH (10 mL). The clear solution was then added to **2·Cl_2** (12.2 mg, 39.2 µmol) in 1:1 H_2O:EtOH (5 mL), and the resulting cloudy solution left to stand at room temperature. Crystals were observed after approximately 1 hr. After two days, the clear needle crystals were isolated by filtration, washed with water (3 mL) and air-dried.

Yield: 14.4 mg (12.3 µmol, 63%).

^{1}H NMR (400 MHz, d_6-DMSO containing a drop of conc. $HCl_{(aq)}$): 9.65 (br. s, 8H), 9.41 (br. s, 8H), 8.05 (s, 16H), 7.59 (d, *J* = 8.1 Hz, 8H) and 7.22–7.29 (m, 8H) ppm.

ATR-IR (*inter alia*): 1007 (B-C stretching) cm^{-1}.

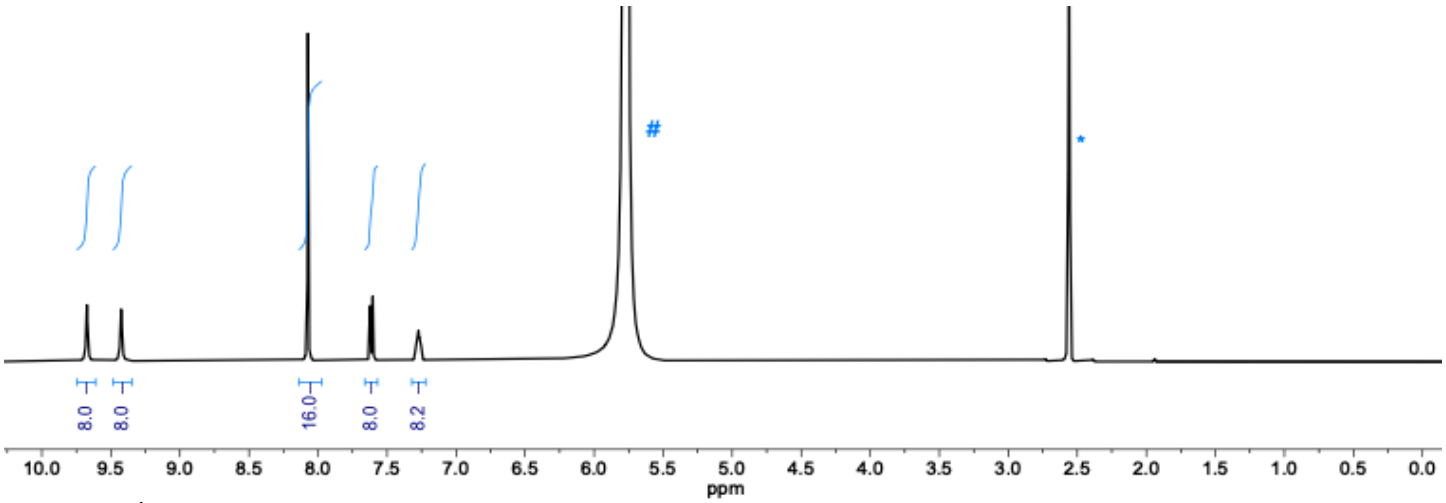

Figure S14. ^{1}H NMR spectrum of acid-digested **Na·2₂·B**; peak labelled * results from incompletely deuterated NMR solvent, peak labelled # results from water (d_6-DMSO containing 1 drop $HCl_{(aq)}$, 400 MHz, 298 K).

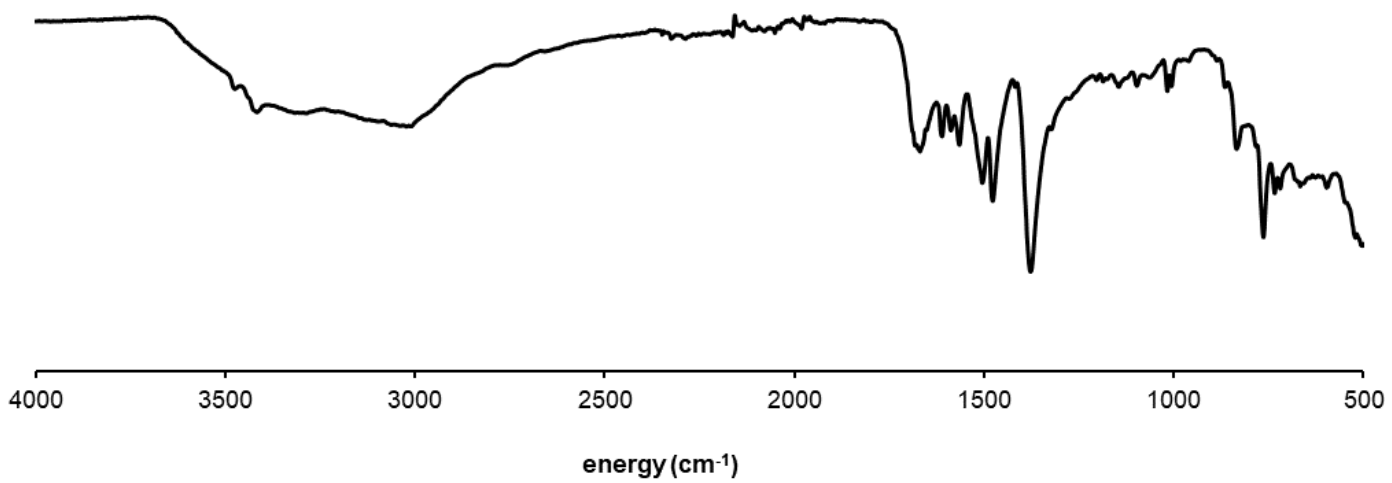

Figure S15. ATR-IR spectrum of **Na·2₂·B**.

The TGA trace of **Na·2₂·B** showed a sharp drop at ~35 °C which we attribute to non-coordinated water molecules (Figure S16). A much slower mass loss is then observed between 50 °C to 220 °C, which we attribute to water molecules coordinated to the sodium cation. Overall a mass lost corresponding to approximately 10 water molecules is observed.

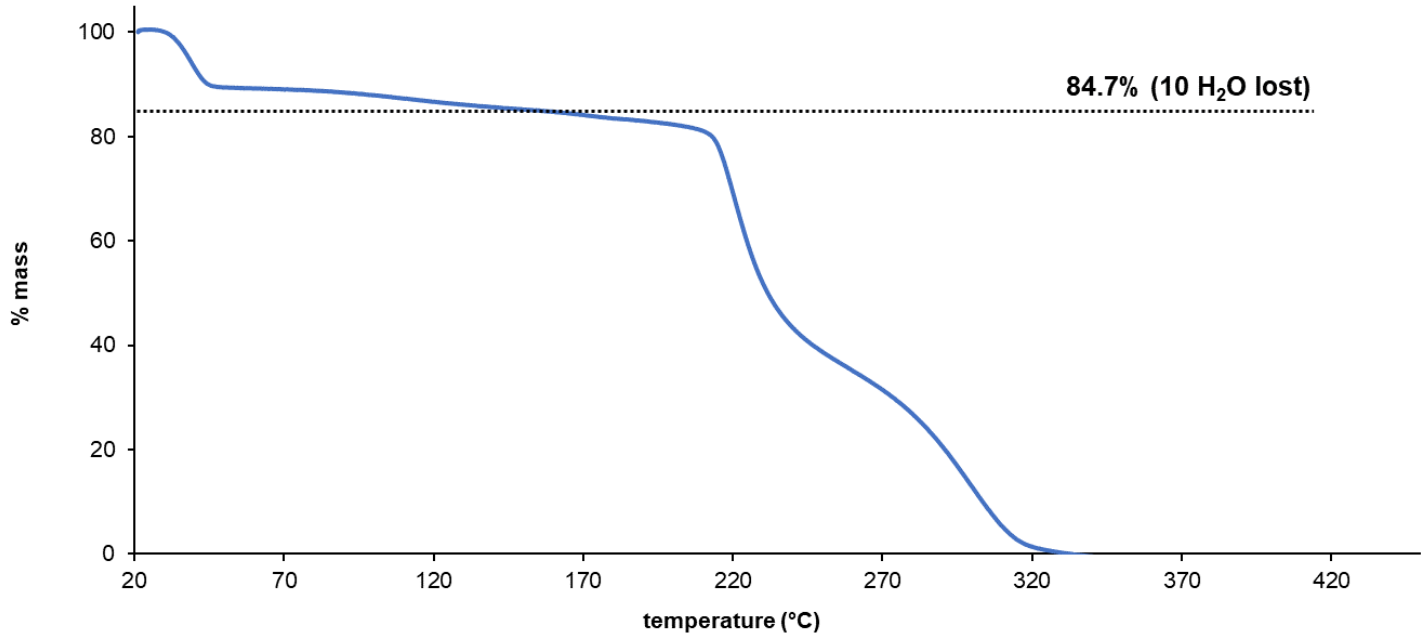

Figure S16. TGA trace of **Na·2₂·B**. The black dotted line indicates the expected mass lost corresponding to water solvents from framework.

The PXRD of **Na·2₂·B** before drying is very poorly crystalline but has a PXRD pattern that matches relatively well with that calculated based on the SCXRD structure (Figure S17), however upon standing for a short period (minutes) the PXRD trace begins to change to a new phase, which we attribute to the compound rearranging as it loses solvent. The PXRD of the framework after drying under mild vacuum corresponds to this new phase.

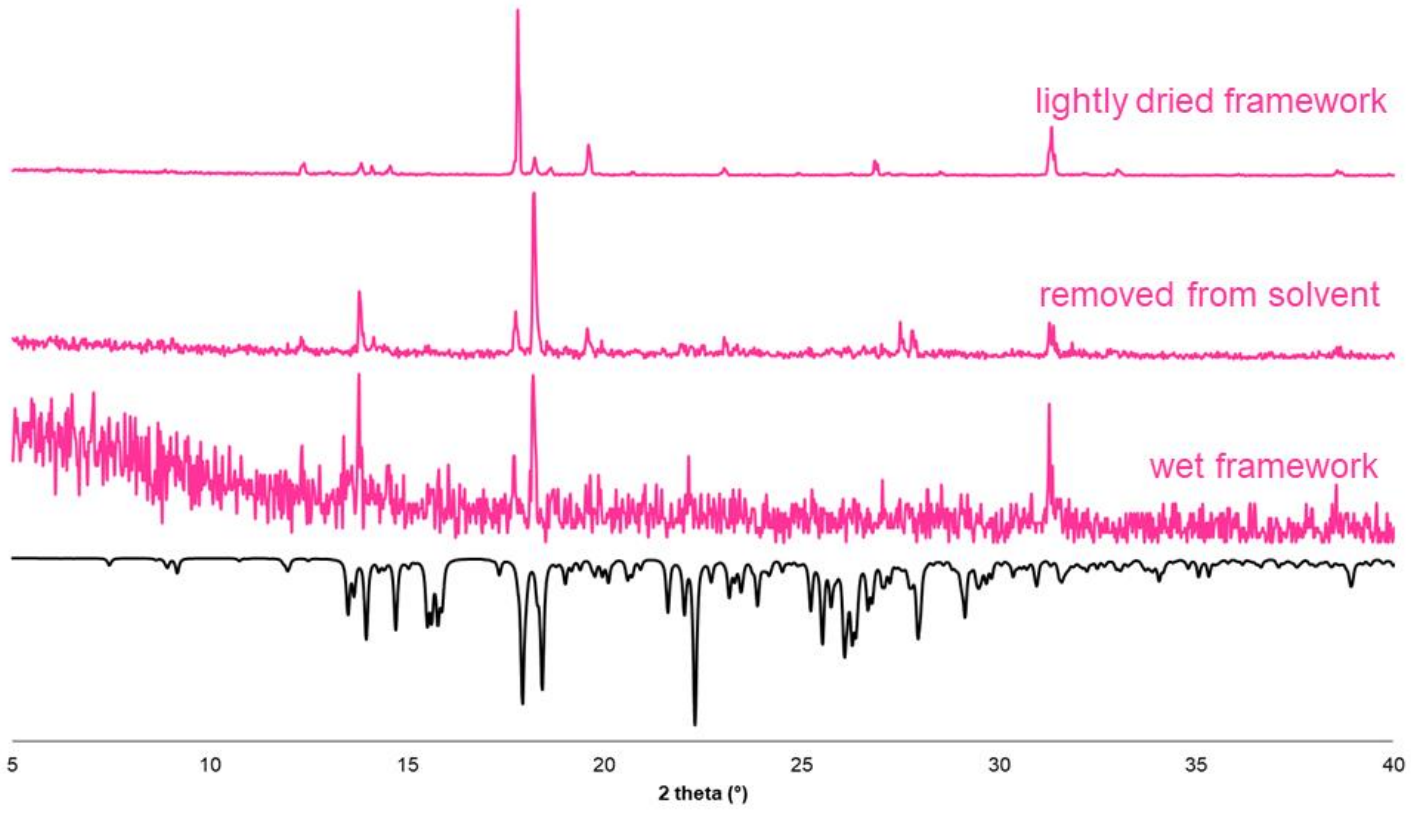

Figure S17. PXRD pattern of **Na·2₂·B** (red) and the respective calculated trace (black) from SCXRD data.

Cation exchange of TBA·$\mathbf{2_2}$·B

Cation exchange crystallisations

For these experiments, crystals of **TBA·$\mathbf{2_2}$·B** (~ 1 mg) were stood in 1.0 M aqueous solutions of LiCl, NaCl, KCl, NH_4Cl, $MgCl_2$ or $CaCl_2$. After two weeks, the crystals were analysed using SCXRD, which showed that cation exchange had occurred with loss of the TBA^+ group and structural transformations to give frameworks containing Li^+, Na^+, K^+, NH_4^+, Mg^{2+} or Ca^{2+} cations.

In the case of the Na^+ containing framework, we collected datasets for both the crystals prepared directly in the presence of a large excess of Na^+ and for crystals of **TBA·$\mathbf{2_2}$·B** that were incubated in 1.0 M $NaCl_{(aq)}$. These two datasets revealed identical structures and so only the higher quality dataset (the crystals prepared directly in the presence of Na^+) is reported here.

Attempts to conduct cation exchange using NaI instead of NaCl were unsuccessful. No crystals were obtained when NaI was incorporated in the initial crystallisation, and incubating **TBA·$\mathbf{2_2}$·B** in NaI led to decomposition of the crystals.

All attempts to obtain frameworks containing tetra-amidinium $\mathbf{1^{4+}}$ and $\mathbf{B^{5-}}$ and cations other than TBA^+, either by incorporating other cations during the initial crystallisation or by incubating **TBA·1·B** in salt solutions, were unsuccessful.

^{1}H NMR experiments

For these experiments, we placed approximately 1 mg of crystals of **TBA·2$_2$·B** in 1 mL 1.0 M $NaCl_{(aq)}$ or $CaCl_{2(aq)}$. After various time intervals (0, 5, 10, 20, 30 and 40 minutes), we isolated the framework by filtration, washed with water (3 mL), and dried. We then digested the framework using DMSO-d_6 containing two drops of concentrated $HCl_{(aq)}$. The solution was then analysed using ^{1}H-NMR spectroscopy (Figure S18).

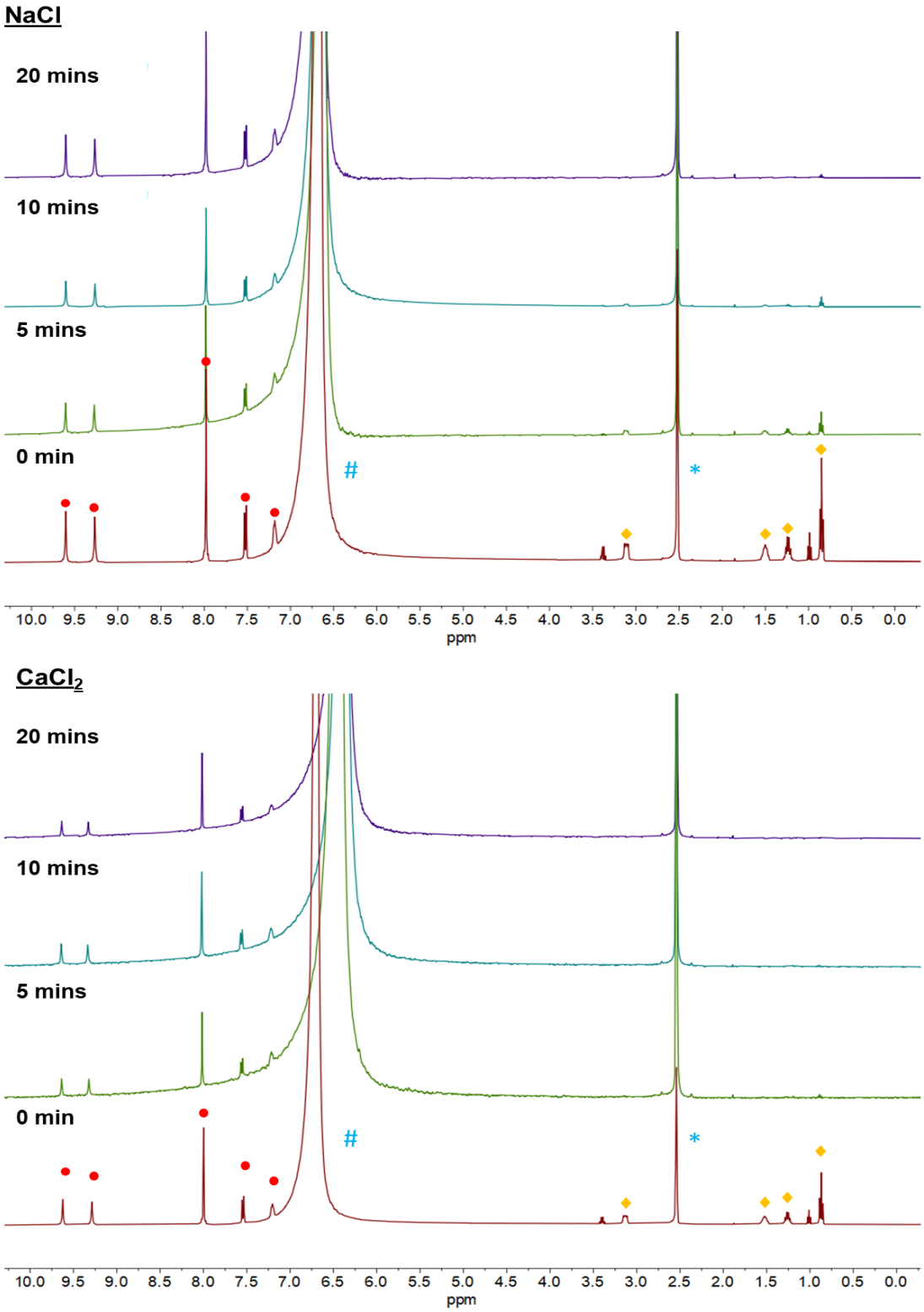

Figure S18. ^{1}H NMR spectra of **TBA·2$_2$·B** after incubation with 1.0 M $NaCl_{(aq)}$ or 1.0 M $CaCl_{2(aq)}$ at different time intervals. Peaks corresponding to $\mathbf{2}^{2+}$ and $\mathbf{B}^{5-}$ are indicated by red circles, peaks corresponding to the TBA cation are indicated by yellow diamonds. The water peak and residual NMR solvent peak are indicated by # and *, respectively.

The TBA^+ peak at 0.93 ppm was integrated and compared to the framework C–H peak at 8.04 ppm, and this was used to calculate the percentage reduction of TBA^+ cation over time as shown in Figure S19.

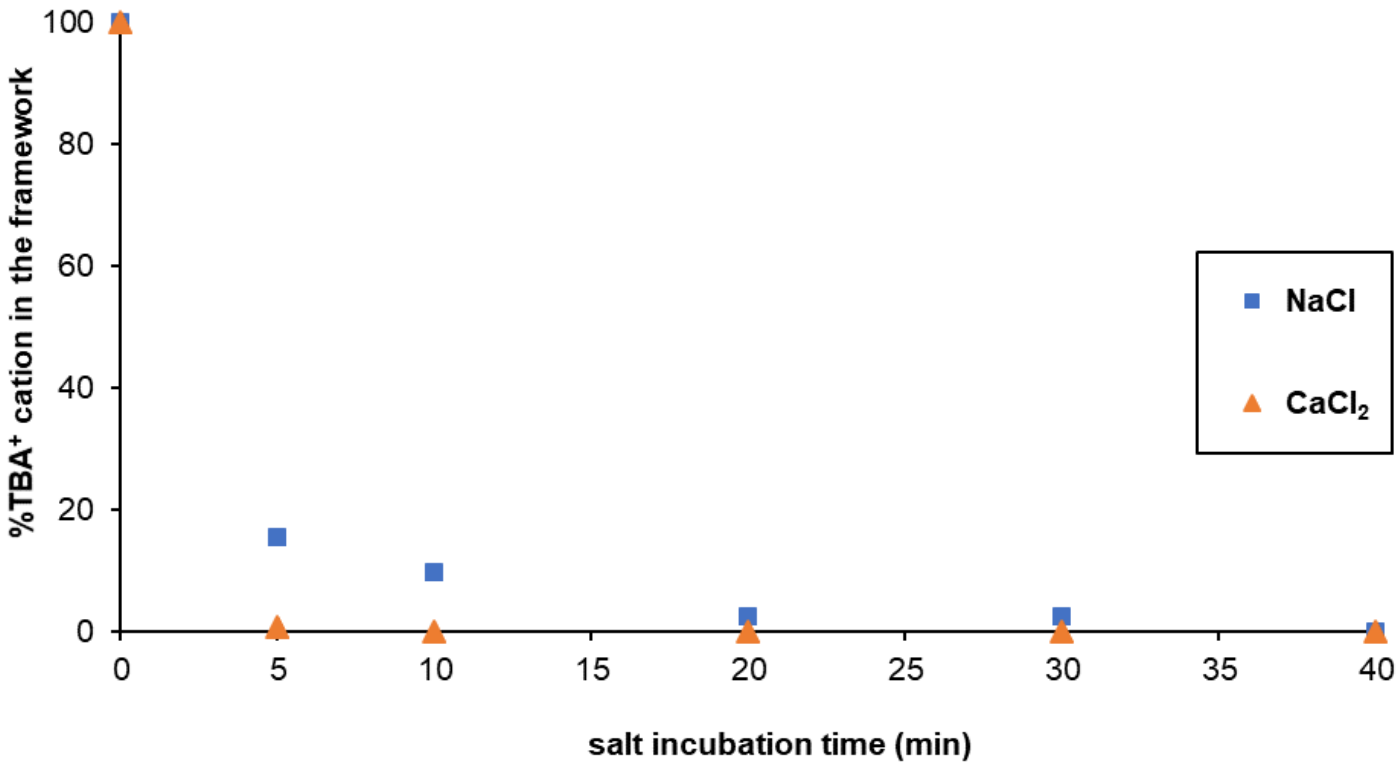

Figure S19. Graph of % TBA cation remaining in **TBA·2$_2$·B** after incubation with 1.0 M $NaCl_{(aq)}$ (blue) or $CaCl_{2(aq)}$ (orange) solutions at different time intervals.

X-ray Crystallography

General remarks

All crystals were mounted at 213 K using a 3D-printed μCHILL[5] cold mounting device prior to single crystal X-ray diffraction studies. Data were collected at either 100 K using the MX2 beamline[6] at the Australian Synchrotron, or at 150 K using Cu Kα radiation on an Agilent SuperNova diffractometer. Raw frame data for synchrotron data were processed using XDS,[7] raw frame data for structures collected using Cu radiation were processed using CrysAlis Pro.[8] Many of the crystal structures contain numerous water molecules; for all structures apart from the low quality structure of **Li·2$_2$·B** we have attempted to locate the hydrogen atoms on these structures as best as we can, however due to the poor diffraction arising from hydrogen atoms these locations should be treated with caution. The structure of **NH$_4$·2$_2$·B** contains NH_4^+ cations disordered about a four-fold rotation axis. The location of the hydrogen atoms on this cation should also be treated with caution.

Details of structure refinements, including thermal ellipsoids plots, are provided on the following pages. Selected crystallographic data are summarised in Table S2. Full crystallographic data in CIF format have been uploaded to the Cambridge Structural Database (CCDC Numbers: 2238927 – 2238935).

Summary of crystallographic data

Table S2. Summary of crystallographic data.

	TBA·1·B [a]	**$2_{2.5}$·B_2**	**TBA·2_2·B** [b]	**Li·2_2·B**	**Na·2_2·B**
Radiation type	synchrotron (λ=0.71075 Å)	Cu Kα (λ=1.54184 Å)	Cu Kα (λ=1.54184 Å)	synchrotron (λ=0.71075 Å)	Cu Kα (λ=1.54184 Å)
Temperature (K)	100	150	150	100	150
Formula	$C_{16}H_{36}N{\cdot}C_{29}H_{32}N_8{\cdot}C_{28}H_{16}BO_8$ [a]	$(C_{14}H_{16}N_4)_{2.5}{\cdot}C_{28}H_{16}O_8{\cdot}(H_2O)_5$	$(C_{16}H_{36}N)_2{\cdot}(C_{14}H_{16}N_4)_4{\cdot}(C_{28}H_{16}BO_8)_2$ [b]	$Li{\cdot}(C_{14}H_{16}N_4)_2{\cdot}C_{28}H_{16}BO_8{\cdot}(H_2O)_{12}$ [c]	$Na{\cdot}(C_{14}H_{16}N_4)_2{\cdot}C_{28}H_{16}BO_8{\cdot}(H_2O)_{10}$
Formula weight	1226.34	1182.06	2428.57	1194.98	1174.98
***a* (Å)**	14.476(3)	14.1697(4)	28.0407(7)	19.427(3)	19.2633(6)
***b* (Å)**	39.955(8)	14.5406(4)	39.4728(15)	19.427(3)	14.7730(5)
***c* (Å)**	16.910(3)	16.0657(5)	18.8173(12)	7.4870(15)	19.7937(7)
***α* (º)**	90	110.045(3)	90	90	90
***β* (º)**	98.23(3)	110.898(3)	103.209(4)	90	92.871(3)
***γ* (º)**	90	96.920(2)	90	90	90
Unit cell volume (Å^3)	9680(3)	2791.70(16)	20276.8(16)	2825.8(10)	5625.8(3)
Crystal system	monoclinic	triclinic	monoclinic	tetragonal	monoclinic
Space group	$P2_1/c$	P–1	$P2_1/c$	P4/n	$P2_1/n$
Z	4	2	4	2	4
Reflections (all)	171987	40019	55310	51440	15878
Reflections (unique)	16936	8003	28883	1622	8008
R_{int}	0.120	0.042	0.070	0.020	0.042
R_1 [$I > 2\sigma(I)$]	0.138	0.039	0.105	0.223	0.080
wR_2 (all data)	0.287	0.101	0.363	0.276	0.220
CCDC number	2238927	2238928	2238929	2238930	2238931

[a] PLATON-SQUEEZE[9] was used. [b] OLEX2 solvent mask[10] was used. [c] Hydrogen atoms on water molecules were unable to be located.

	K·2_2·B	**NH_4·2_2·B**	**$Mg_{0.5}$·2_2·B**	**$Ca_{0.5}$·2_2·B**
Radiation type	synchrotron (λ=0.71075 Å)	Cu Kα (λ=1.54184 Å)	Cu Kα (λ=1.54184 Å)	Cu Kα (λ=1.54184 Å)
Temperature (K)	100	150	150	150
Formula	$K_2{\cdot}(C_{14}H_{16}N)_4{\cdot}(C_{28}H_{16}BO_8)_2{\cdot}(H_2O)_{20}$	$NH_4{\cdot}(C_{14}H_{16}N)_2{\cdot}C_{28}H_{16}BO_8{\cdot}(H_2O)_{10}$	$Mg{\cdot}(C_{14}H_{16}N)_4{\cdot}(C_{28}H_{16}BO_8)_2{\cdot}(H_2O)_{22}$	$Ca_0{\cdot}(C_{14}H_{16}N)_4{\cdot}(C_{28}H_{16}BO_8)_2{\cdot}(H_2O)_{22}$
Formula weight	2382.16	1170.04	2364.33	2380.08
***a* (Å)**	19.618(3)	19.6061(8)	19.5332(5)	19.5879(12)
***b* (Å)**	19.618(3)	19.6061(8)	19.5332(5)	19.5879(12)
***c* (Å)**	14.977(3)	15.0982(9)	15.1579(4)	15.0908(14)
***α* (º)**	90	90	90	90
***β* (º)**	90	90	90	90
***γ* (º)**	90	90	90	90
Unit cell volume (Å^3)	5764(2)	5803.7(6)	5783.4(3)	5790.1(9)
Crystal system	tetragonal	tetragonal	tetragonal	tetragonal
Space group	P4/n	P4/n	P4/n	P4/n
Z	2	4	2	2
Reflections (all)	77857	10575	10335	8219
Reflections (unique)	5864	5603	5706	4134
R_{int}	0.104	0.059	0.054	0.157
R_1 [$I > 2\sigma(I)$]	0.059	0.088	0.075	0.104
wR_2 (all data)	0.180	0.246	0.203	0.355
CCDC number	2238932	2238933	2238934	2238935

Details of individual refinements

Structure of **TBA·1·B**

Crystals were small and poorly-diffracting and so this structure was collected using microfocus synchrotron radiation using the MX2 beamline at the Australian Synchrotron.[6] It was solved using SUPERFLIP[11] and refined within the CRYSTALS suite.[12] The structure crystallises in the monoclinic space group $P2_1/c$ and the asymmetric unit contains one TBA^+ cation, one $\mathbf{1}^{4+}$ cation and one $\mathbf{B}^{5-}$ anion. There are also large areas of poorly resolved electron density, which appear to correspond to disordered water molecules. These could not be modelled sensibly and so PLATON-SQUEEZE[9] was used to include this electron density in the model. One phenyl amidinium group appears to be waving back and forth. Attempts to model this over two positions were unsuccessful. Instead, restraints were applied to the bond lengths and thermal and vibrational parameters of this group. One phenyl carboxylate groups is disordered: this was modelled over two positions with restraints applied to bond lengths and angles as well as thermal and vibrational parameters of the disordered atoms.

A thermal ellipsoid plot is shown in Figure S20 and the packing of the structure is shown in Figure S21.

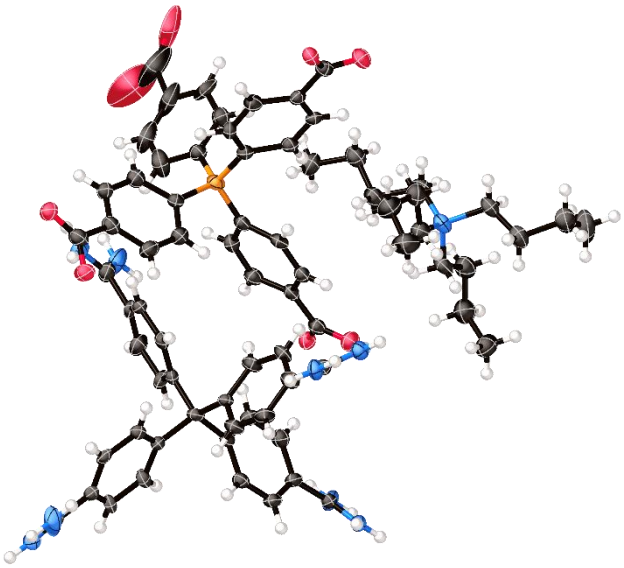

Figure S20. Thermal ellipsoid plot showing the asymmetric unit of **TBA·1·B**; ellipsoids shown at 50% probability level. PLATON-SQUEEZE was used,[9] only one position of disorder is shown.

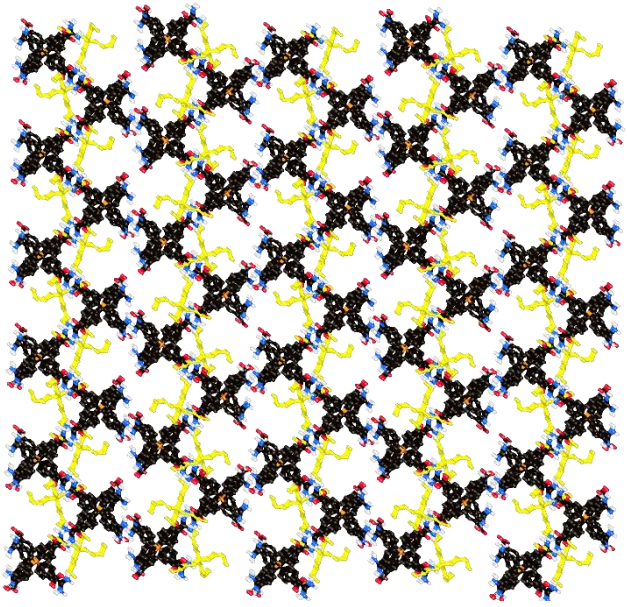

Figure S21. Single crystal structure of **TBA·1·B**. PLATON-SQUEEZE was used,[9] only one position of disorder is shown, C–H hydrogen atoms are omitted for clarity. TBA cations are coloured yellow.

Structure of $\mathbf{2}_{2.5}\cdot\mathbf{B}$

This structure was collected using Cu radiation. It was solved using SHELXT[13] and refined using OLEX2.[10] Crystals were relatively poorly diffracting and no diffraction data could be obtained beyond 0.9 Å. Despite this, the structure refines smoothly and it was not necessary to use any crystallographic restraints. The structure crystallises in the triclinic space group P-1 and the asymmetric unit contains two and a half molecules of $\mathbf{2}^{2+}$, one $\mathbf{B}^{5-}$ anion and five water molecules. A mixture of hydrogen bonding motifs are present, and the structure is relatively densely packed.

A thermal ellipsoid plot is shown in Figure S22 and the packing of the structure is shown in Figure S23.

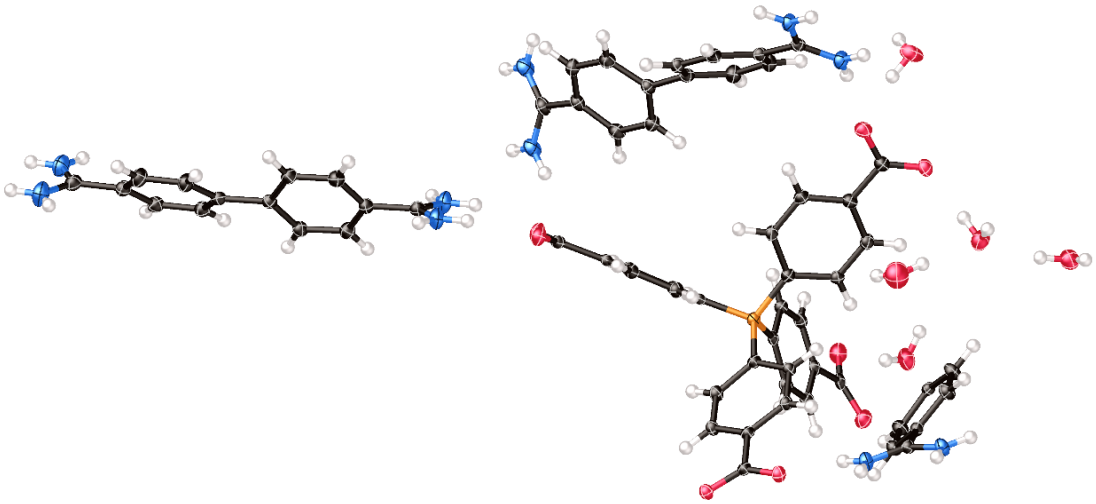

Figure S22. Thermal ellipsoid plot showing the asymmetric unit of $\mathbf{2}_{2.5}\cdot\mathbf{B}$; ellipsoids shown at 50% probability level.

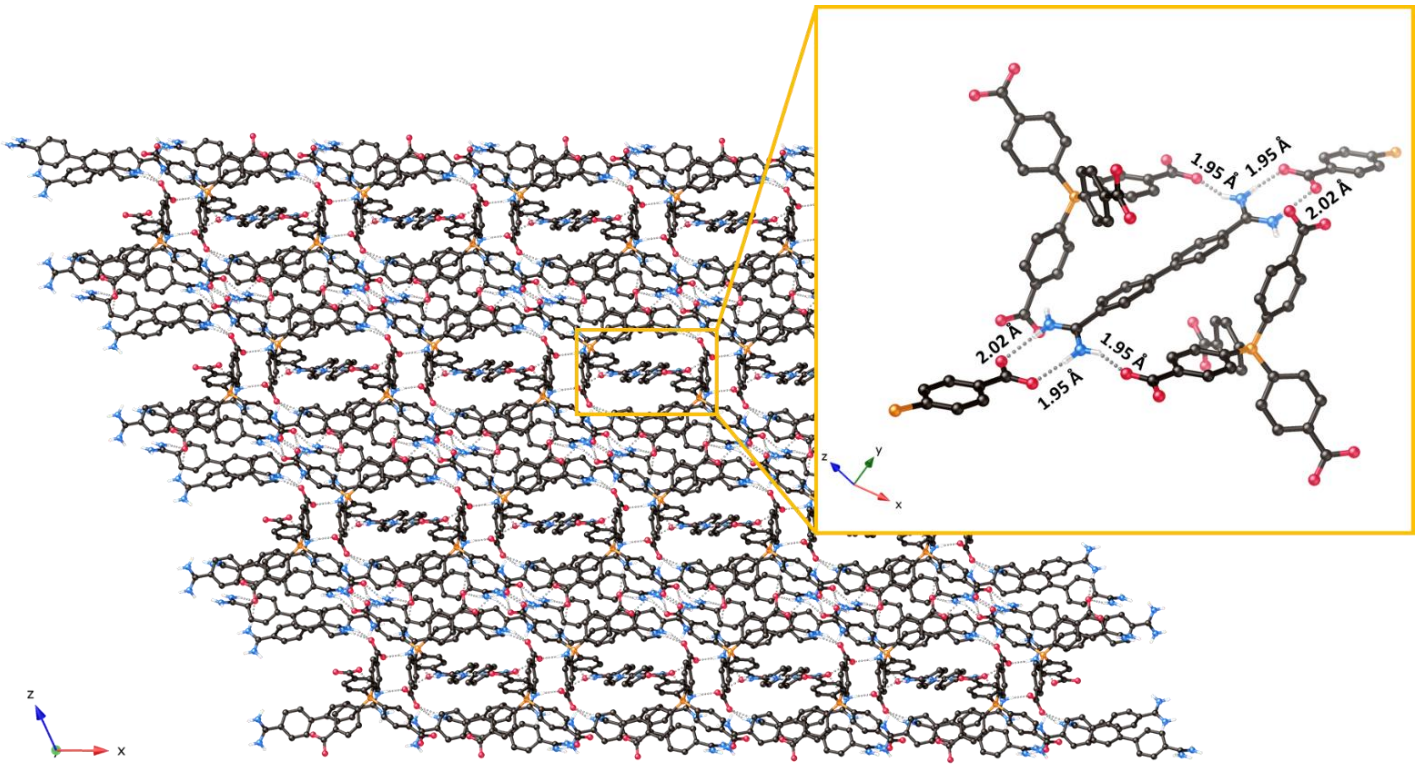

Figure S23. Single crystal structure of $\mathbf{2}_{2.5}\cdot\mathbf{B}$. The structure showed in a yellow box illustrates the hydrogen bonding interactions. C–H hydrogen atoms are omitted for clarity.

Structure of TBA·2_2·B

This structure was collected using Cu radiation. It was solved using SHELXT[13] and refined using OLEX2.[10] Crystals were relatively poorly diffracting and no diffraction data could be obtained beyond 0.9 Å. Despite this, the structure refines relatively smoothly. The structure crystallises in the monoclinic space group $P2_1/c$ and the asymmetric unit contains four molecules of $\mathbf{2}^{2+}$, two $\mathbf{B}^{5-}$ anions and two TBA cations as well as a large region of diffuse electron density that appears to arise from poorly-resolved solvent molecules. These could not be modelled so the OLEX2 solvent mask feature[10] was used to include this electron density in the refinement. One of the TBA^+ cations was relatively poorly-behaved and so DFIX and SIMU restraints were used to achieve a chemically sensible refinement. There is positional disorder of the terminal carbon atom of one of the butyl chains; this was modelled over two positions (occupancies: 50:50).

A thermal ellipsoid plot is shown in Figure S24 and the packing of the structure is shown in Figure 2 of the main text.

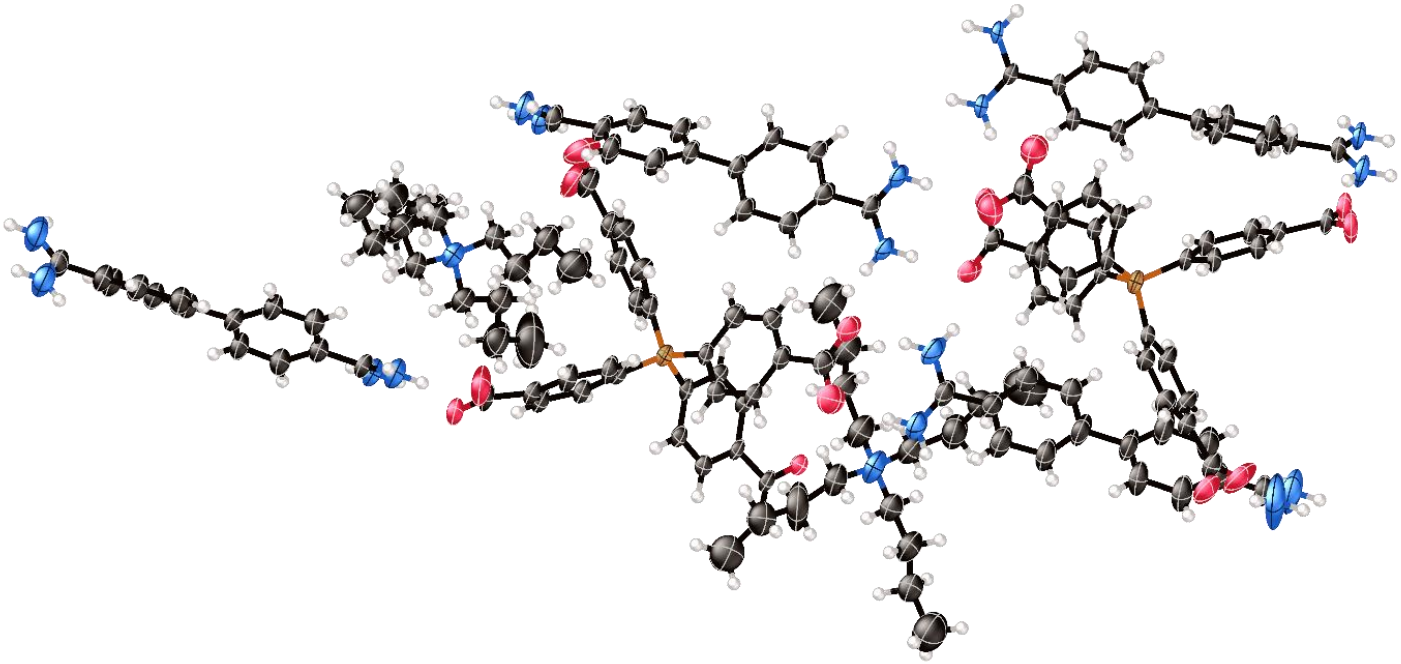

Figure S24. Thermal ellipsoid plot showing the asymmetric unit of **TBA·2_2·B**; ellipsoids shown at 50% probability level. Only one position of the disordered TBA^+ cation is shown. The OLEX2 solvent mask feature was used.[10]

Structure of Li·2_2·B

Crystals were small and poorly-diffracting and so this structure was collected using microfocus synchrotron radiation using the MX2 beamline at the Australian Synchrotron.[6] Despite the use of synchrotron radiation, no data could be obtained beyond a resolution of ~ 1.05 Å. The structure was solved using SHELXT[13] and refined within the CRYSTALS suite.[12] The structure crystallises in the tetragonal space group P4/n and the asymmetric unit contains one quarter of a Li^+ cation, one half of a $\mathbf{2}^{2+}$ cation, one quarter of a $\mathbf{B}^{5-}$ anion and three water molecules.

The data for this structure are of very low quality data and as a result the structure should be viewed with considerable caution, although we note that the **overall framework structure is very similar to the related structures published in this paper, which are based on higher quality data**. Due to the poor quality of the data, it was necessary to add restraints to all bond lengths and all thermal and vibrational ellipsoid parameters as well as nearly all bond angles. It is possible that some or all of the water molecules should be refined as partial occupancy or positionally disordered, but due to the low quality of the data, no attempt was made to model this. No hydrogen atoms are included on these water molecules due to the poor quality of the data.

A thermal ellipsoid plot is shown in Figure S25 and the packing of the structure is shown in Figure S26.

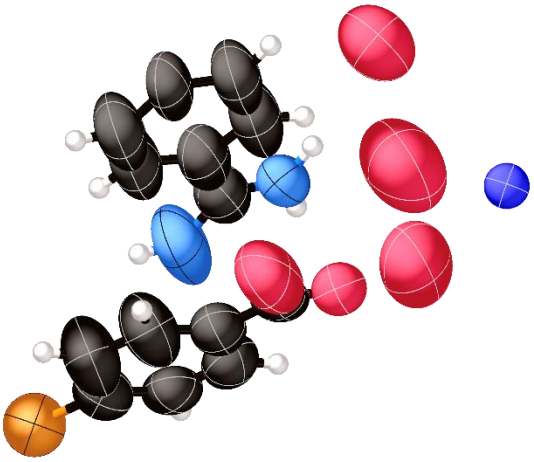

Figure S25. Thermal ellipsoid plot showing the asymmetric unit of **Li·2_2·B**; ellipsoids shown at 50% probability level.

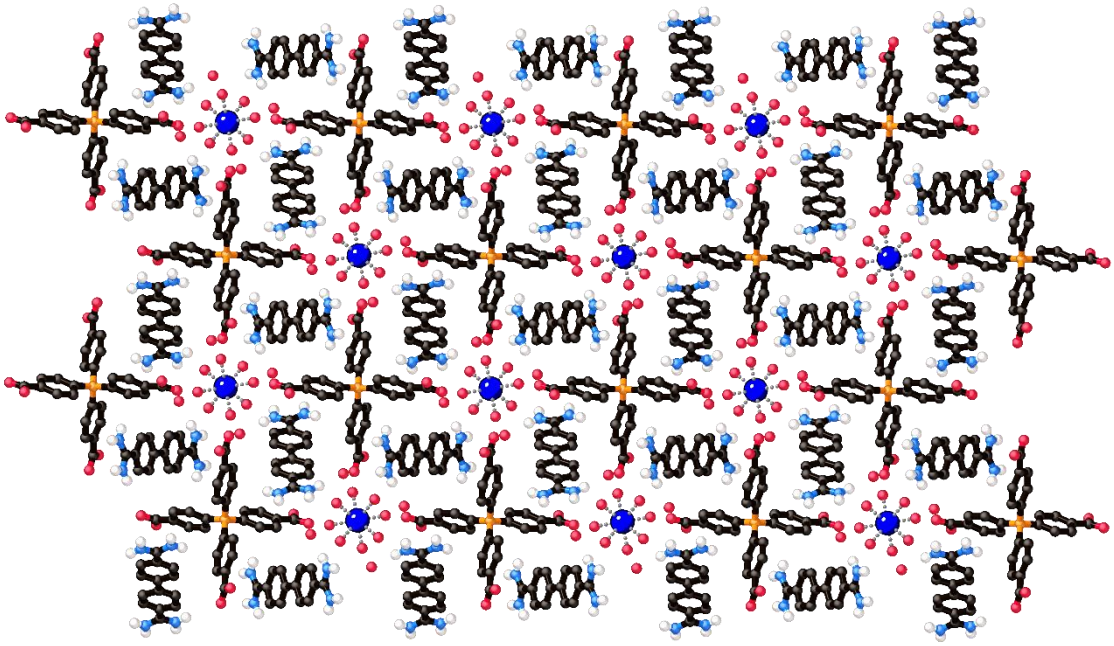

Figure S26. Single crystal structure of **Li·2_2·B**, C–H hydrogen atoms are omitted for clarity.

Structure of Na·2_2·B

This structure was collected using Cu radiation. It was solved using SHELXT[13] and refined using OLEX2.[10] Crystals were relatively poorly diffracting and no diffraction data could be obtained beyond 0.9 Å. Despite this, the structure refines relatively smoothly. The structure crystallises in the monoclinic space group $P2_1/n$ and the asymmetric unit contains one Na^+ cation, two $\mathbf{2}^{2+}$ cations and one $\mathbf{B}^{5-}$ anion and a total of ten water molecules. Six of these water molecules are coordinated to the Na^+ cation, while the remaining four are uncoordinated. There is positional disorder of some water molecules. It was necessary to add restraints (DFIX, DANG, SIMU) to some water hydrogen atoms to achieve a chemically sensible refinement.

A thermal ellipsoid plot is shown in Figure S27 and the packing of the structure is shown in Figure S28.

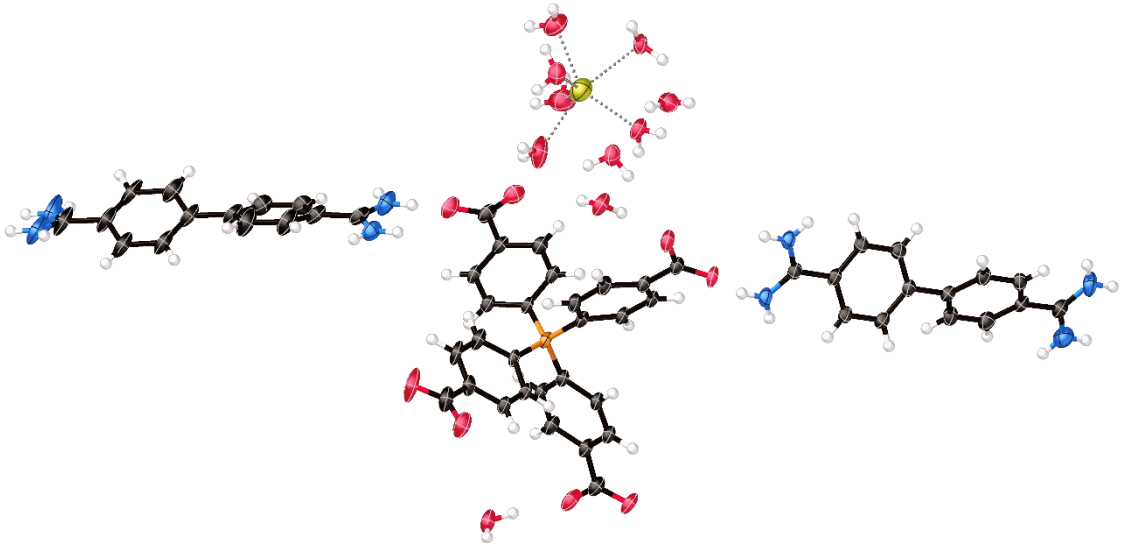

Figure S27. Thermal ellipsoid plot showing the asymmetric unit of **Na·2_2·B**; ellipsoids shown at 50% probability level.

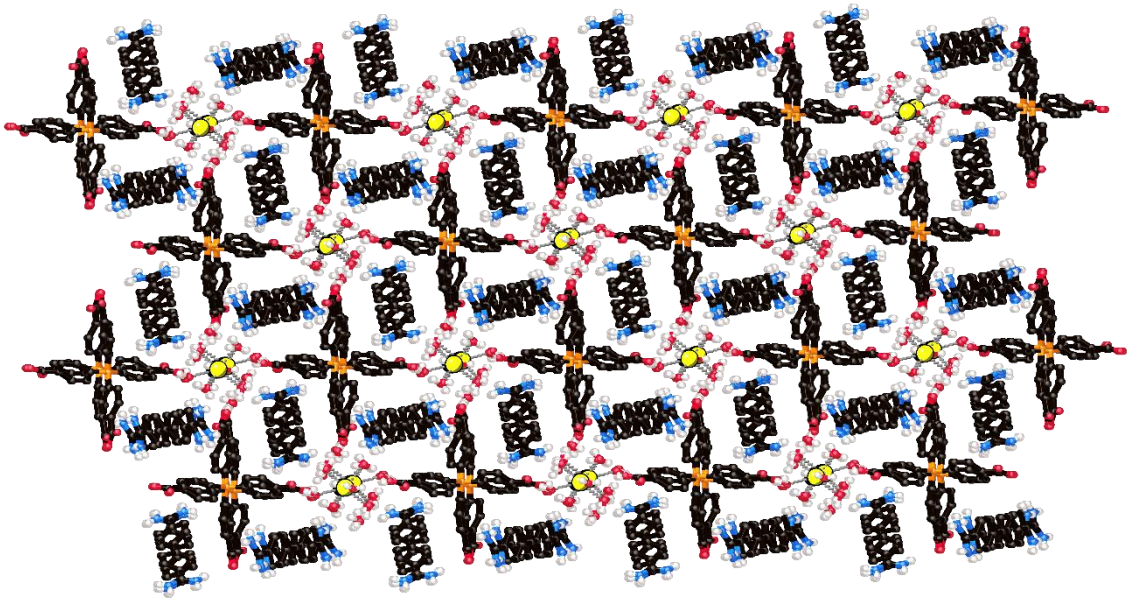

Figure S28. Single crystal structure of **Na·2_2·B**.

Structure of K·2$_2$·B

Crystals were small and poorly-diffracting and so this structure was collected using microfocus synchrotron radiation at the MX2 beamline at the Australian Synchrotron.[6] It was solved using SHELXT[13] and refined using OLEX2.[10] The structure refines smoothly and no crystallographic restraints were necessary. The structure crystallises in the tetragonal space group P4/n and the asymmetric unit contains two quarter K^+ cations, one $\mathbf{2}^{2+}$ cation and two quarter $\mathbf{B}^{5-}$ anions. There are a total of five water molecules, one of which is disordered over two positions (occupancies: 0.5:0.5).

A thermal ellipsoid plot is shown in Figure S29 and the packing of the structure is shown in Figure S30.

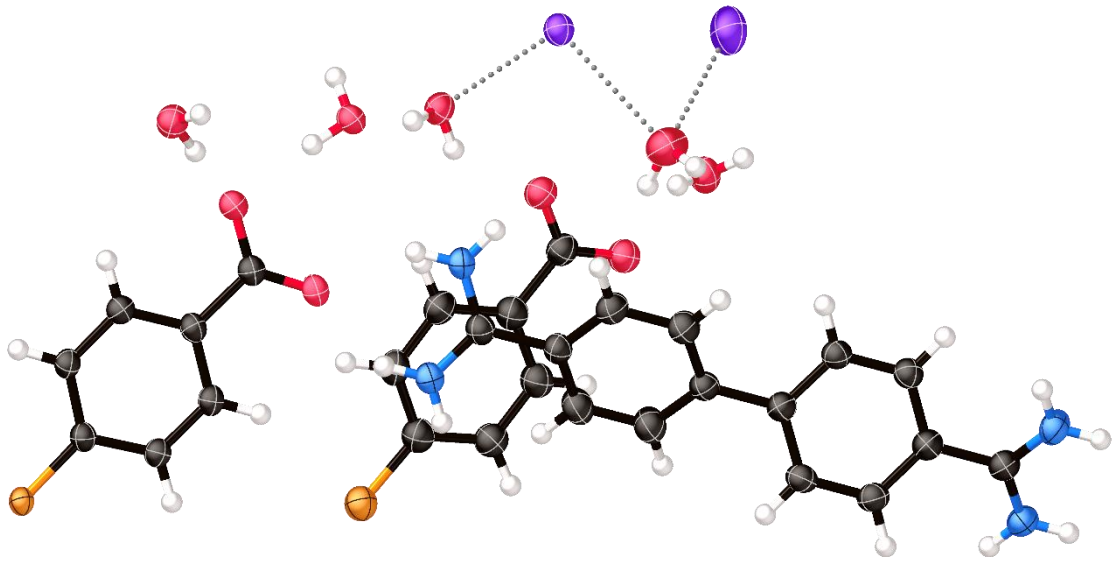

Figure S29. Thermal ellipsoid plot showing the asymmetric unit of **K·2$_2$·B**; ellipsoids shown at 50% probability level. Only one position of the disordered water molecule is shown.

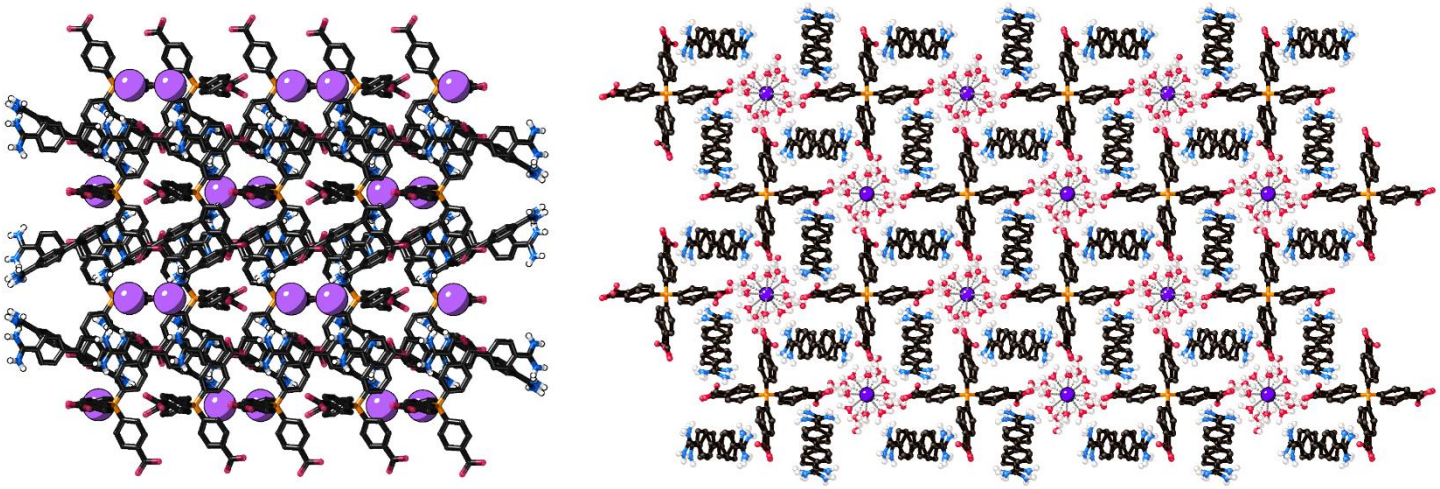

Figure S30. Two views of the single crystal structure of **K·2$_2$·B**. C–H hydrogen atoms are omitted for clarity. Only one position of the disordered water molecule is shown.

The potassium cations exists as a water-bridged dimer (Figure S31). As shown in the Figure, the dimer is very asymmetric with K1 forming relatively short contacts to four terminal water molecules (K···O = 2.796 Å) and longer contacts to four bridging water molecules (K···O = 3.036 Å). K2 forms short contacts to the bridging water molecules (K···O = 2.745 Å) but very long (possibly insignificant) contacts to four terminal water molecules (this water molecule is disordered over two positions, the closest position has K···O = 3.928 Å).

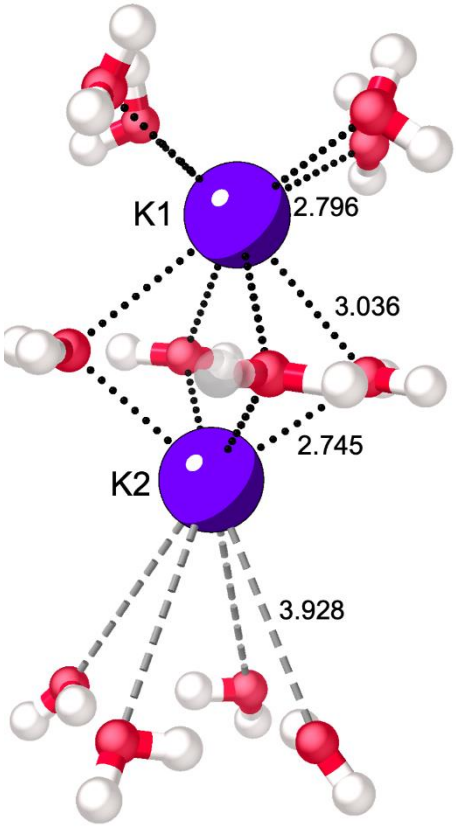

Figure S31. Part of single crystal structure of **K·2₂·B** showing the water-bridge K^+ dimer. Bond lengths for each crystallographically-independent interaction are shown in Å. Only one position of the disordered water molecules (those 3.928 Å from K2) is shown.

Structure of $NH_4 \cdot 2_2 \cdot B$

This structure was collected using Cu radiation. It was solved using SHELXT[13] and refined using OLEX2.[10] The structure refines smoothly and apart from restraints on ammonium N–H bond lengths no crystallographic restraints were necessary. The structure crystallises in the tetragonal space group P4/n and the asymmetric unit contains two quarter NH_4^+ cations (disordered about a four-fold rotation axis), one $\mathbf{2}^{2+}$ cation and two quarter $\mathbf{B}^{5-}$ anions. There are a total of five water molecules.

A thermal ellipsoid plot is shown in Figure S32 and the packing of the structure is shown in Figure S33.

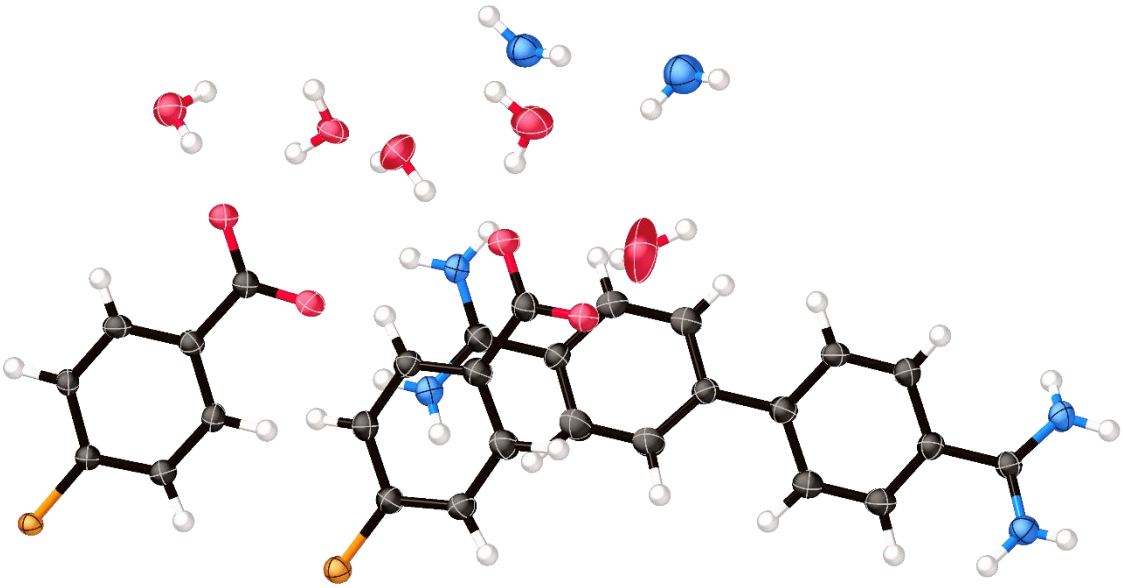

Figure S32. Thermal ellipsoid plot showing the asymmetric unit of $NH_4 \cdot 2_2 \cdot B$; ellipsoids shown at 50% probability level.

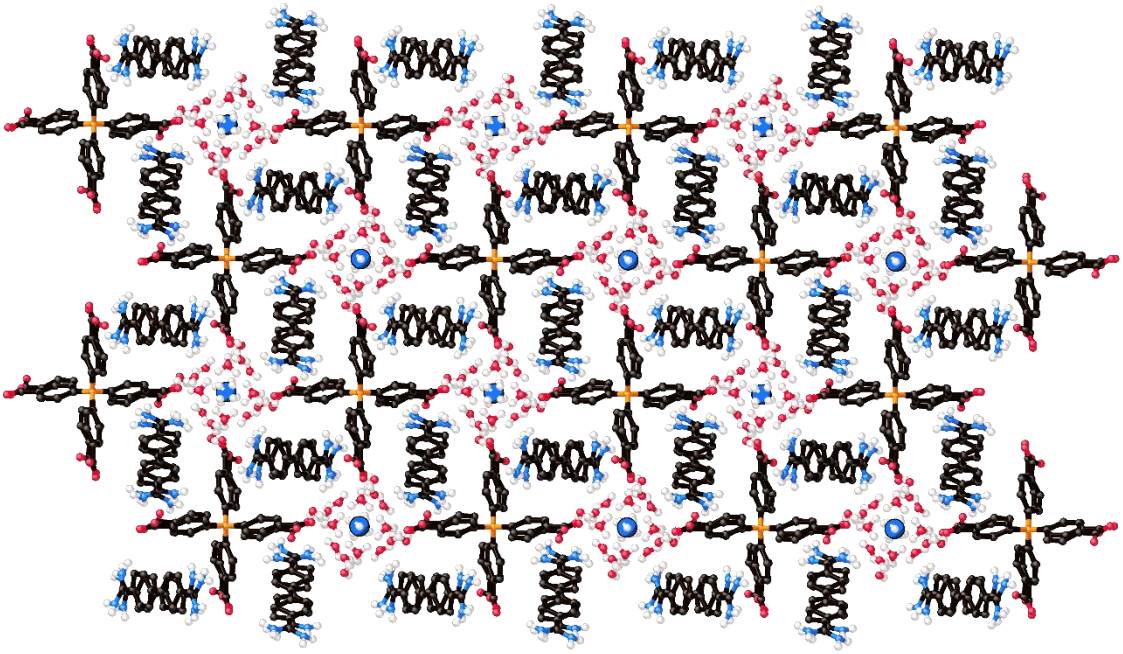

Figure S33. Single crystal structure of $NH_4 \cdot 2_2 \cdot B$. C–H hydrogen atoms are omitted for clarity.

Structure of $Mg_{0.5}$·2_2·B

This structure was collected using Cu radiation. It was solved using SHELXT[13] and refined using OLEX2.[10] The structure refines smoothly and no crystallographic restraints were necessary. The structure crystallises in the tetragonal space group P4/n and the asymmetric unit contains one quarter of a Mg^{2+} cation (situated on a four-fold rotation axis), one $\mathbf{2}^{2+}$ cation and two quarter $\mathbf{B}^{5-}$ anions. There are a total of five and a half water molecules: 1.5 of these are coordinated to the Mg^{2+} cation in an octahedral arrangement located on the four-fold rotation axis with the hydrogen atoms of these molecules disordered about this axis. The remaining four water molecules are uncoordinated and one of these is positionally disordered (occupancies: 0.5:0.5).

A thermal ellipsoid plot is shown in Figure S34 and the packing of the structure is shown in Figure S35.

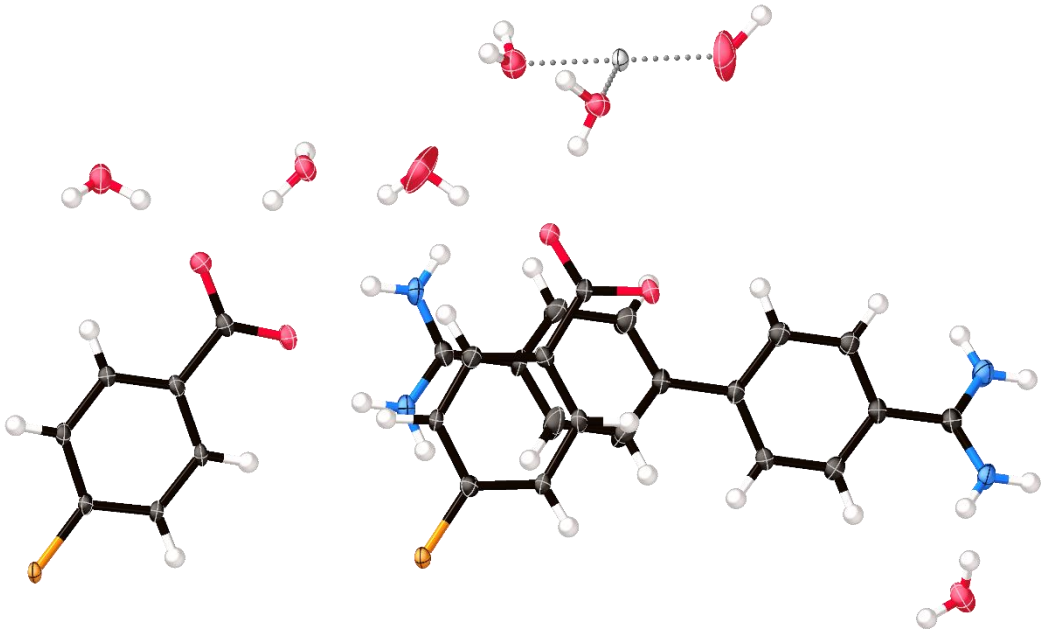

Figure S34. Thermal ellipsoid plot showing the asymmetric unit of **$Mg_{0.5}$·2_2·B**; ellipsoids shown at 50% probability level. Only one position of disordered water molecules is shown.

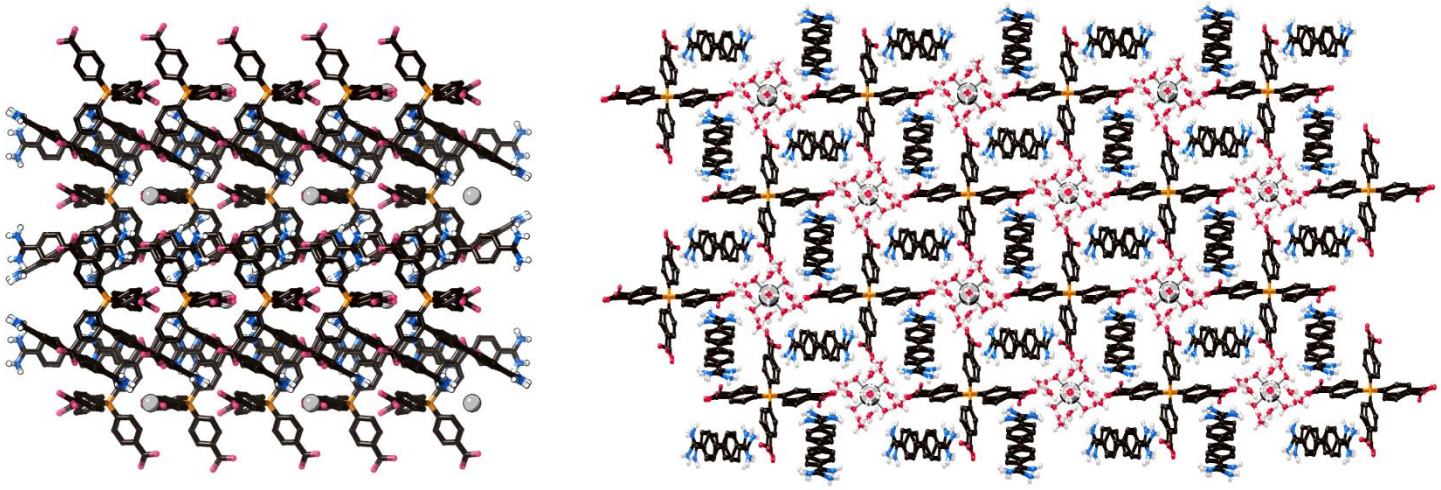

Figure S35. Two views of the single crystal structure of **$Mg_{0.5}$·2_2·B**. C–H hydrogen atoms are omitted for clarity. Only one position of disordered water molecules is shown.

Structure of $Ca_{0.5}$·2_2·B

This structure was collected using Cu radiation. It was solved using SHELXT[13] and refined using OLEX2.[10] The data are weak and of relatively low quality and no reflection data could be obtained beyond a resolution of 0.9 Å. Despite the weak data, the structure refines smoothly. The structure crystallises in the tetragonal space group P4/n and the asymmetric unit contains one quarter of a Ca^{2+} cation (situated on a four-fold rotation axis), one $\mathbf{2}^{2+}$ cation and two quarter $\mathbf{B}^{5-}$ anions. There are a total of five and a half water molecules: 1.5 of these are coordinated to the Ca^{2+} cation in an octahedral arrangement located on the four-fold rotation axis with the hydrogen atoms of these molecules disordered about this axis. The remaining four water molecules are uncoordinated and one of these is positionally disordered (occupancies: 0.75:0.25). It was necessary to apply restraints to two C–C and one C–O bond lengths to achieve sensible geometries.

A thermal ellipsoid plot is shown in Figure S36 and the packing of the structure is shown in Figure S37.

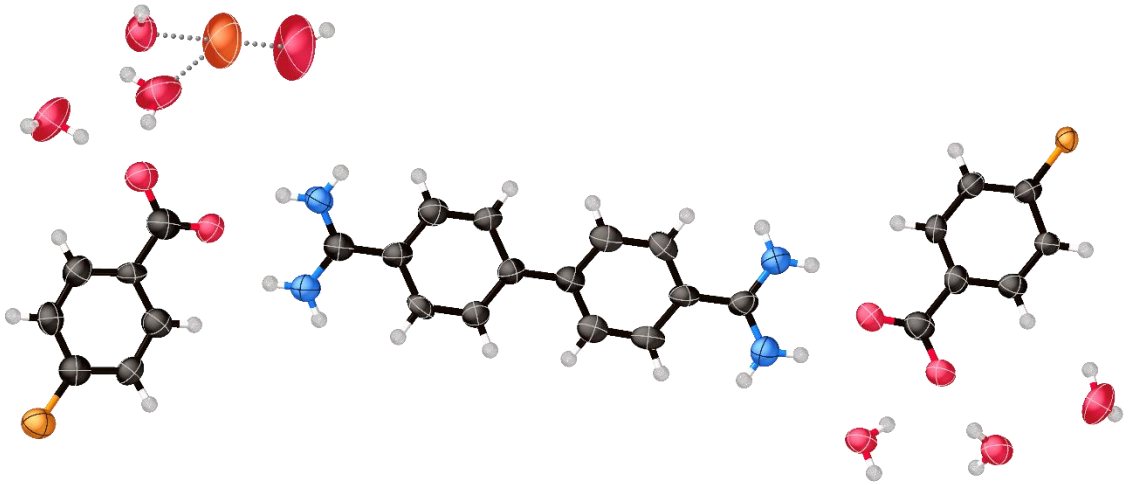

Figure S36. Thermal ellipsoid plot showing the asymmetric unit of **$Ca_{0.5}$·2_2·B**; ellipsoids shown at 50% probability level. Only one position of disordered water molecules is shown.

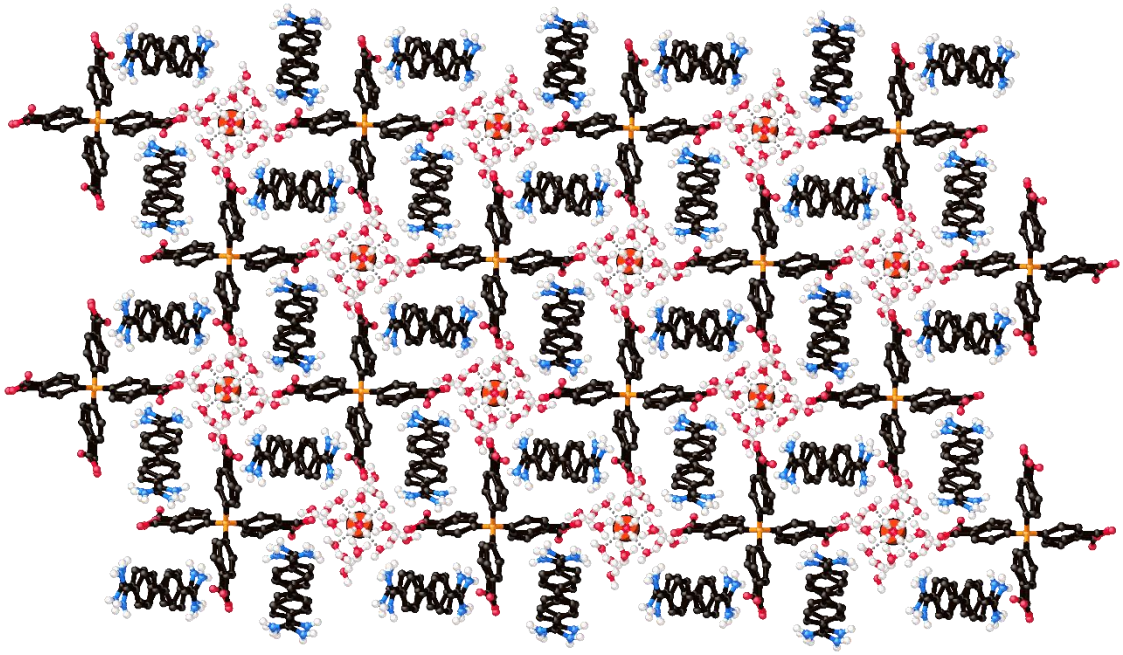

Figure S37. Single crystal structure of **$Ca_{0.5}$·2_2·B**. C–H hydrogen atoms are omitted for clarity. Only one position of disordered water molecules is shown.

Methylene blue and crystal violet adsorption

Structures of MB^+ and CV^+

The structures of MB^+ and CV^+ are provided in Figure S38. Both dyes were used as their chloride salts.

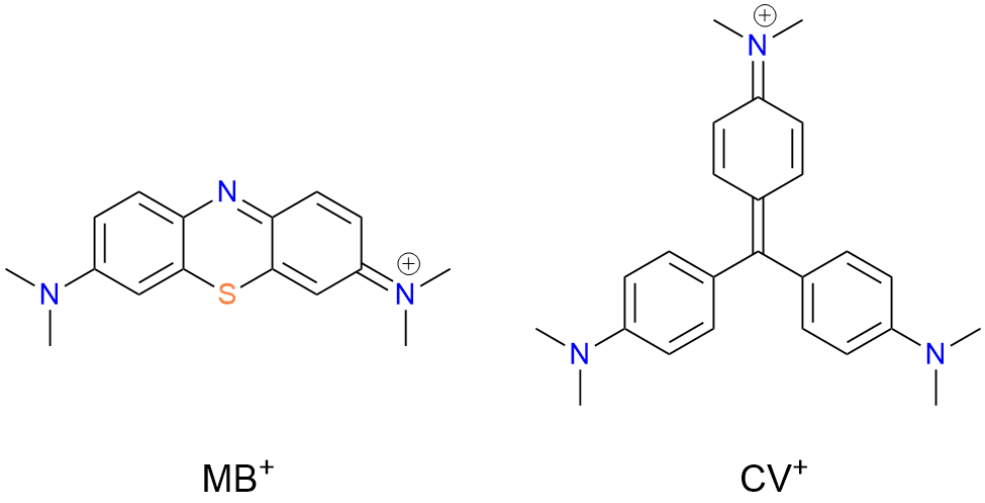

Figure S38. Structures of MB^+ and CV^+.

UV Vis spectroscopy (28 μM, 1.0 equivalent framework)

Initially, crystals of **$2_{2.5}$·B**, **TBA·2_2·B** and **Na·2_2·B** were stood in 28 μM aqueous solutions of MB^+ or CV^+ at a 1:1 molar ratio of framework:MB^+. At different time intervals, approximately 1 mL of the solution was removed from the vial and a UV-Vis spectrum recorded. This was then immediately returned to the vial after analysis. The reduction in intensity of the peak at 660 nm and 590 nm for MB^+ and CV^+, respectively, was used to measure the concentration of dye left in the solution (Figure S39 – S41). All measurements were conducted in triplicate.

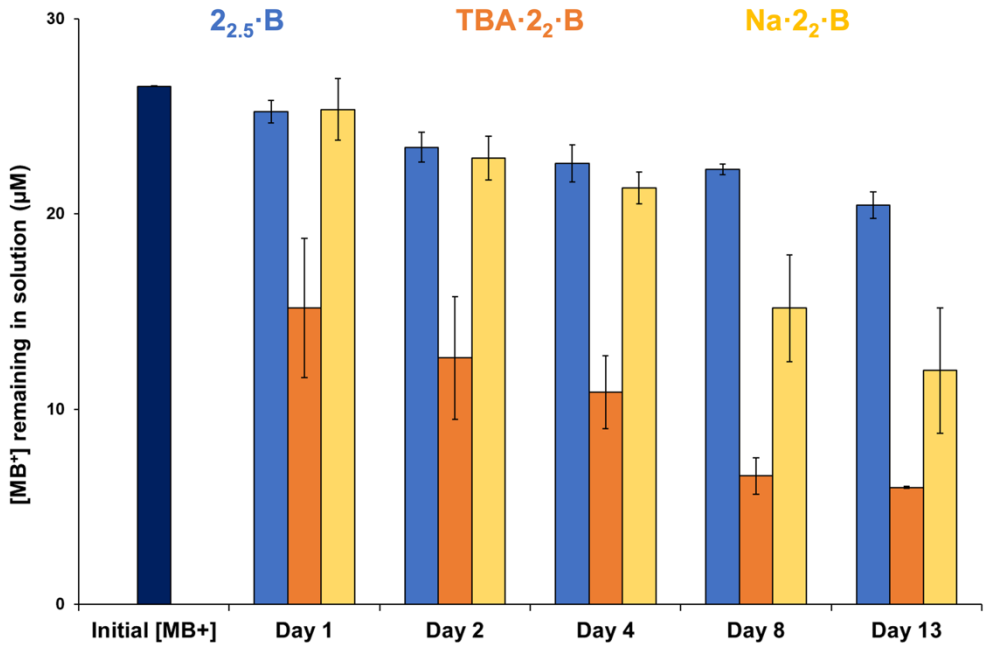

Figure S39. Graphs showing concentration of MB^+ solution at different incubation time intervals with **$2_{2.5}$·B** (blue), **TBA·2_2·B** (orange), and **Na·2_2·B** (yellow). Measurements were conducted in triplicate, error bars represent the standard deviation of these experiments.

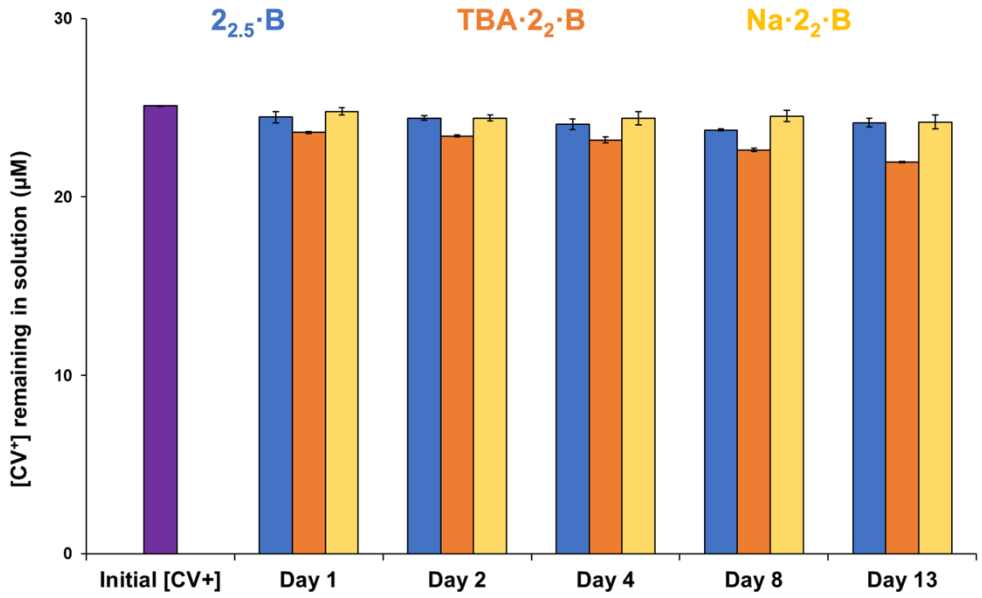

Figure S40. Graphs showing concentration of CV^+ solution at different incubation time intervals with **$2_{2.5}$·B** (blue), **TBA·2_2·B** (orange), and **Na·2_2·B** (yellow). Measurements were conducted in triplicate, error bars represent the standard deviation of these experiments.

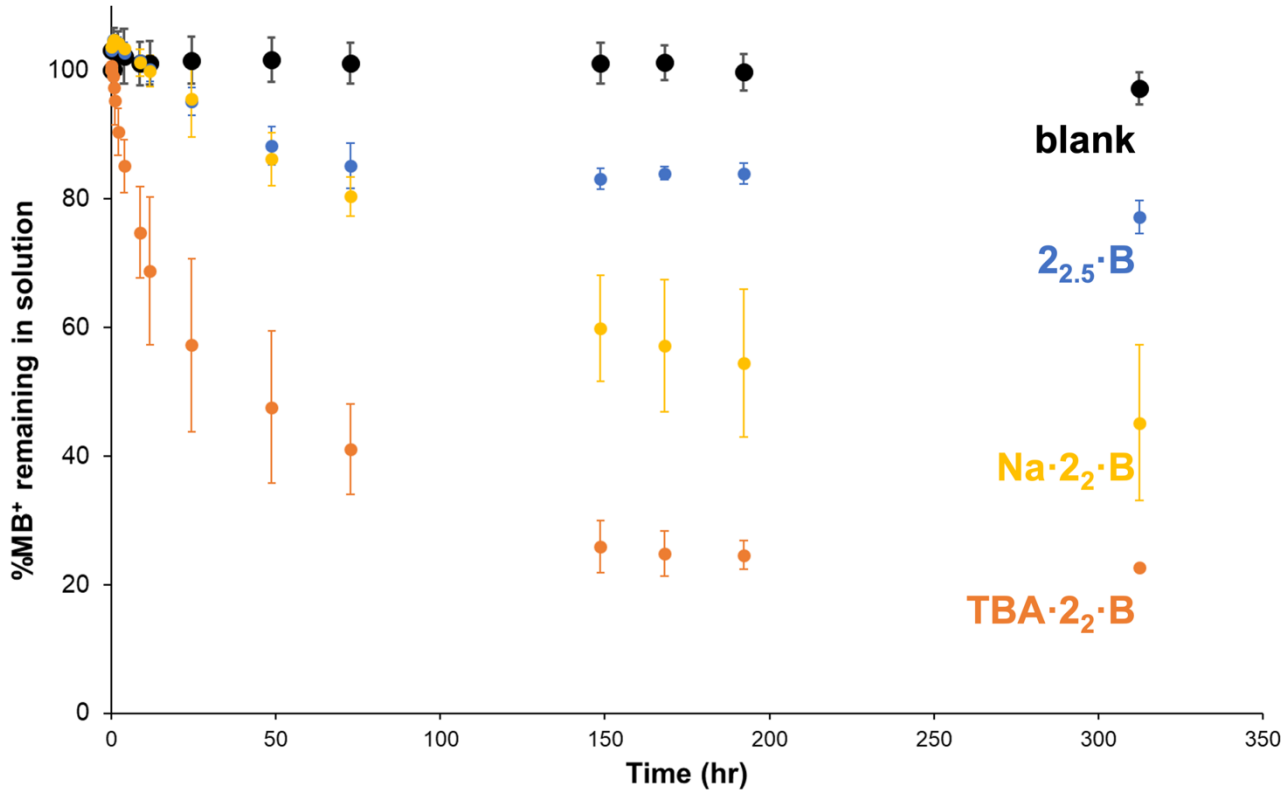

Figure S41. Graphs showing % of MB^+ remaining in water at different incubation time intervals with **$2_{2.5}$·B** (blue), **TBA·2_2·B** (orange), and **Na·2_2·B** (yellow). Measurements were conducted in triplicate, error bars represent the standard deviation of these experiments (initial concentration: 28 μM).

UV Vis spectroscopy (55 µM, 1.0 equivalent framework)

Increasing the concentration of MB^+ binding solution from 28 µM to 55 µM increased the rate of MB^+ adsorption (Figures S42 and S43), however the total amount of MB^+ removed at 55 µM was similar to that at 28 µM (~ 80%).

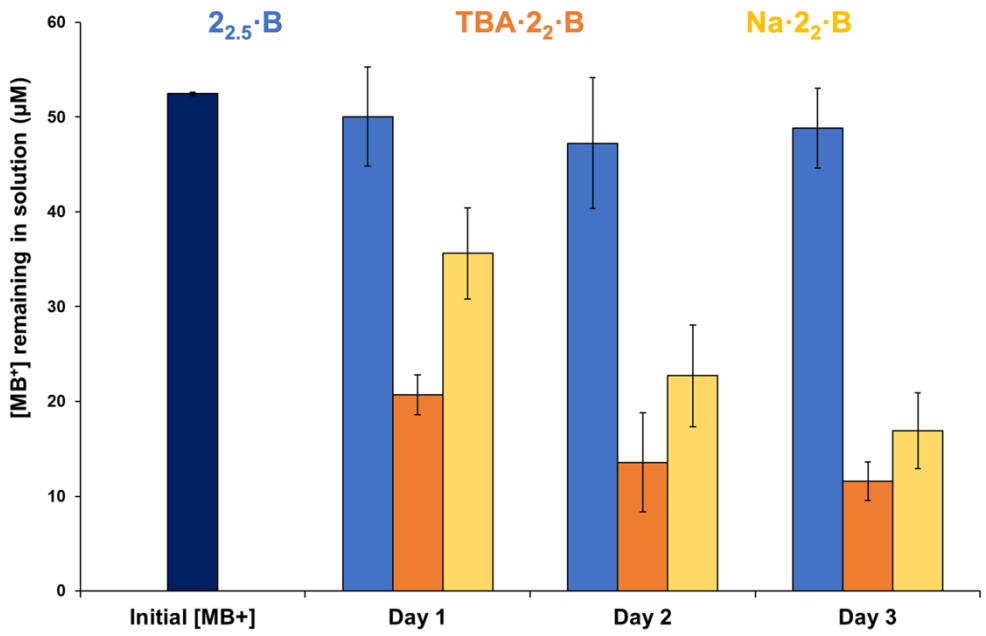

Figure S42. Graphs showing concentration of MB^+ solution at different incubation time intervals with **$2_{2.5}$·B** (blue), **TBA·2_2·B** (orange), and **Na·2_2·B** (yellow). Measurements were conducted in triplicate, error bars represent the standard deviation of these experiments.

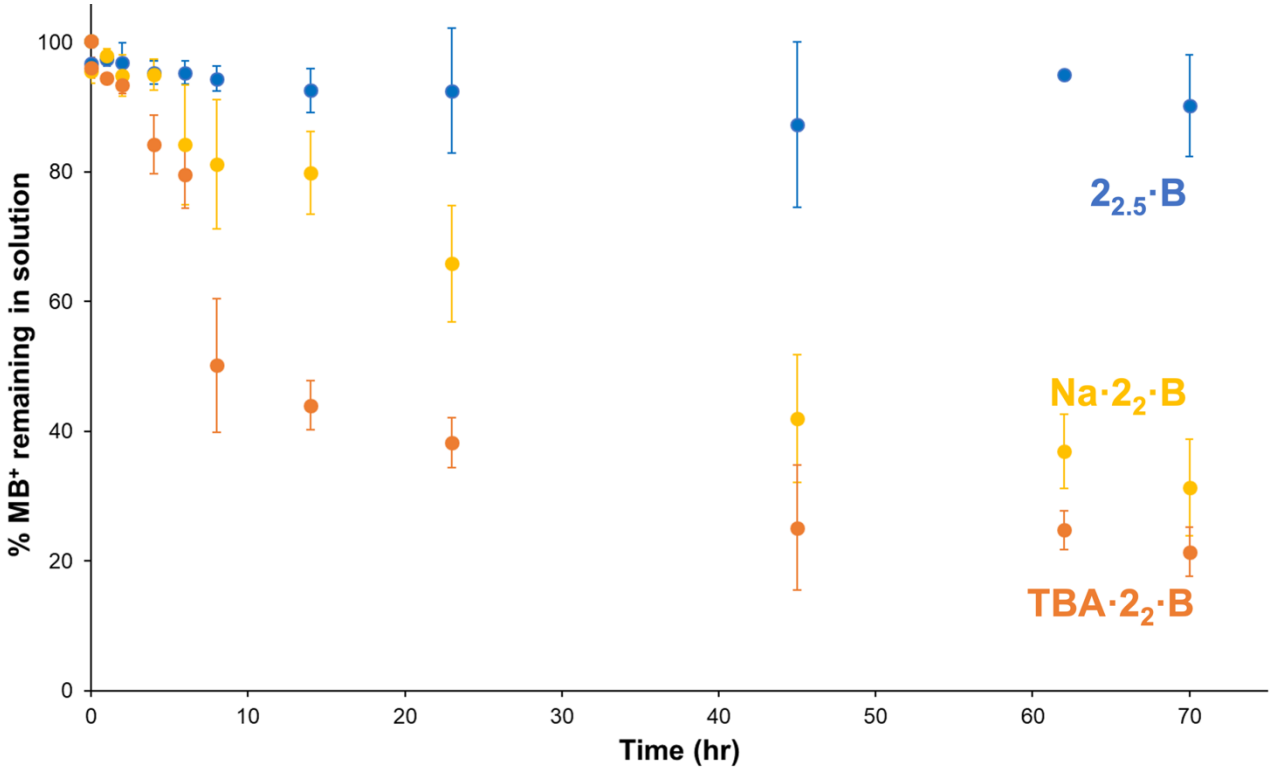

Figure S43. Graphs showing % of MB^+ remaining in water at different incubation time intervals with **$2_{2.5}$·B** (blue), **TBA·2_2·B** (orange), and **Na·2_2·B** (yellow). Measurements were conducted in triplicate, error bars represent the standard deviation of these experiments (initial concentration: 55 µM).

UV Vis spectroscopy (1.5 and 2.0 equivalents framework)

When a small excess of the insoluble framework **TBA·2₂·B** was used, nearly all MB^+ was removed within 1 day. At an initial MB^+ concentration of 28 μM and using 1.5 or 2.0 equivalents of framework, ~95% was removed. At a higher initial dye concentration (55 μM), ~98% was removed. These data are represented graphically in Figure S44.

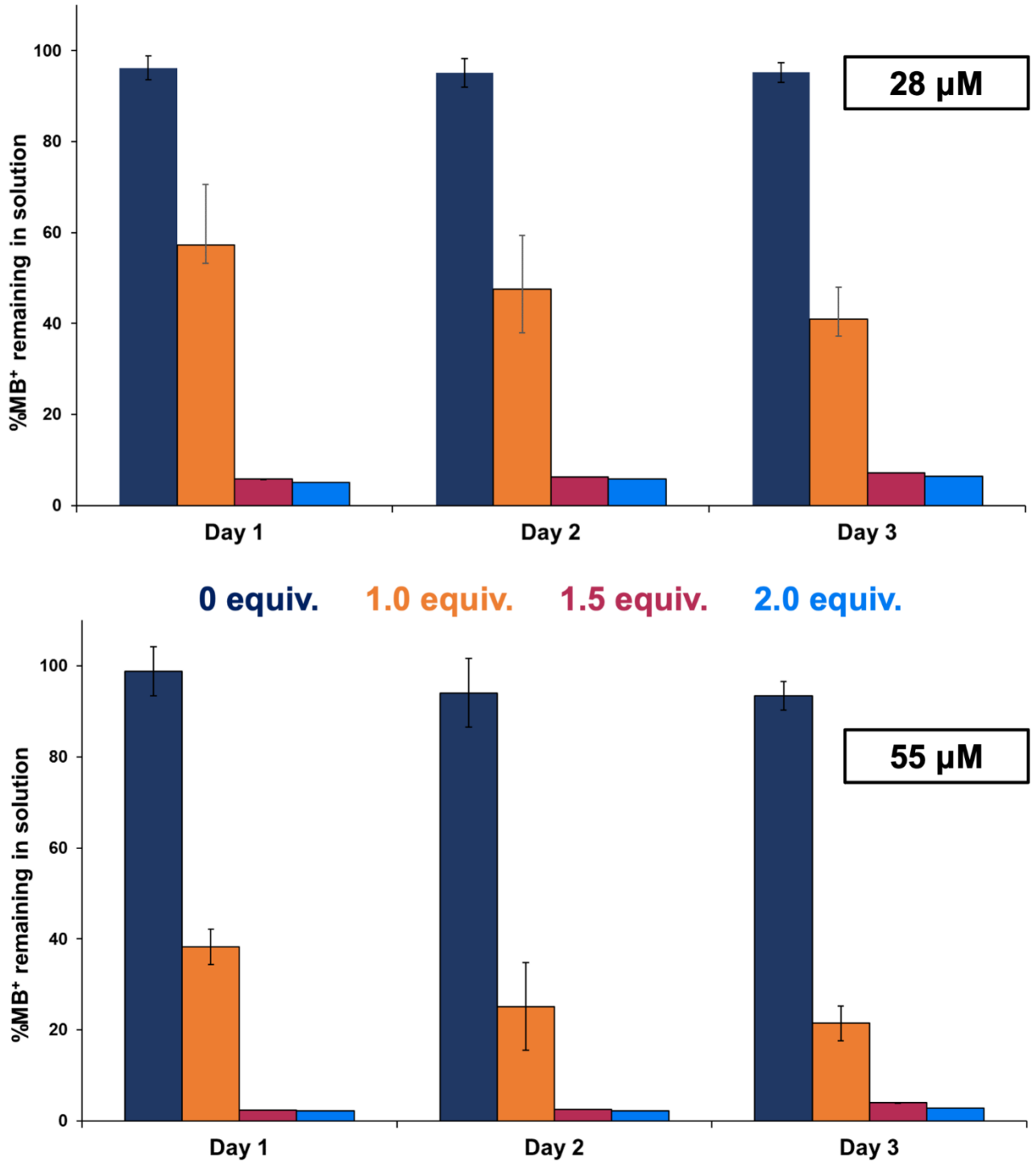

Figure S44. Graphs showing % MB^+ remaining in water at time intervals after incubation with 0 (navy), 1.0 (orange), 1.5 (maroon) or 2.0 (light blue) molar equivalents of **TBA·2₂·B** starting at either 28 or 55 μM MB^+.

Photographs

Photographs of aqueous MB^+ solutions after incubation for five days with 0, 1.0 or 2.0 molar equivalents of **TBA·2₂·B** are shown in Figure S45.

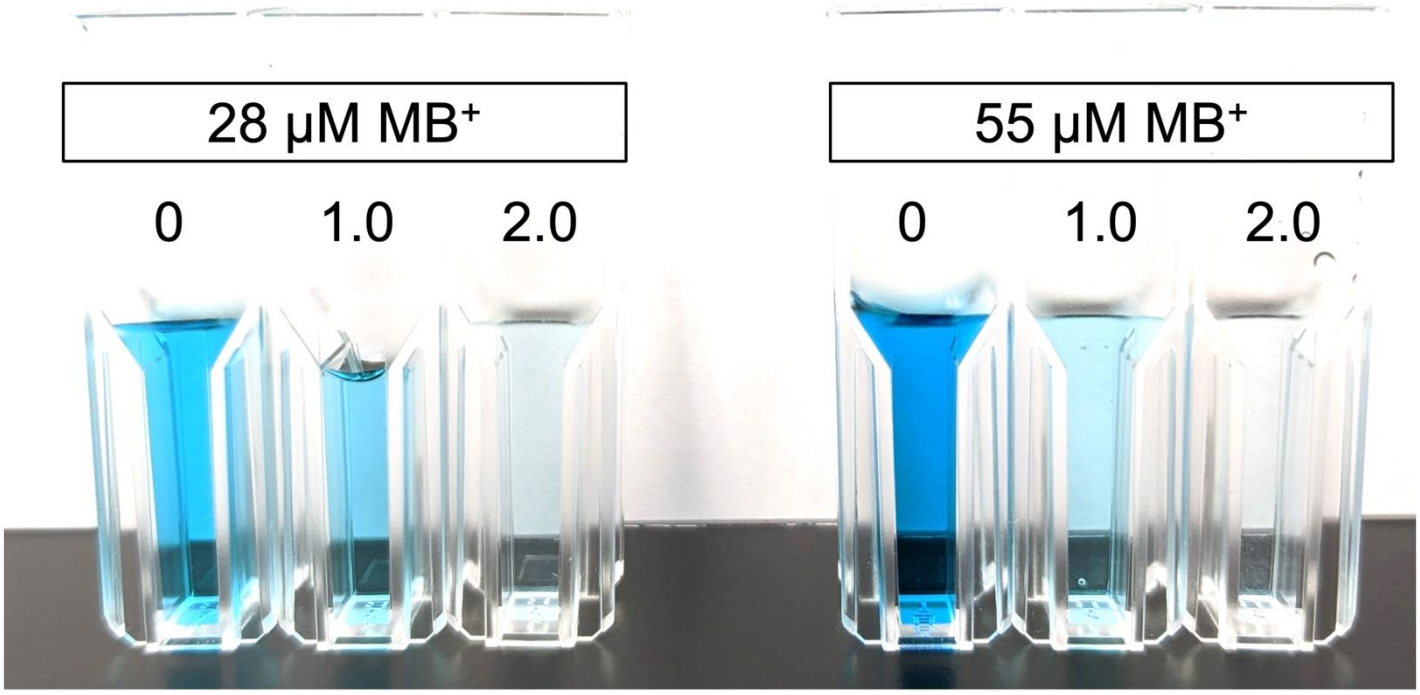

Figure S45. Photographs of aqueous MB^+ solutions containing 0, 1.0 or 2.0 molar equivalents of **TBA·2₂·B** after incubation for five days.

^{1}H NMR spectroscopy

In order to determine the amount of MB^+ and TBA^+ in the crystals of **TBA·2$_2$·B** after two weeks incubation in 28 µm MB^+, we isolated the crystals by filtration, washed them with water, and then dissolved them using DMSO-d_6 containing a drop of concentrated $HCl_{(aq)}$. The resulting solution was then analysed by ^{1}H NMR spectroscopy (Figure S46). The spectrum clearly shows the presence of MB^+ peaks (marked as blue triangles) and TBA^+ peaks (marked as yellow diamonds). The integration of the MB^+ methyl peak at 3.38 ppm and - TBA^+ methyl peak at 0.93 ppm were compared to estimate the ratio of the two compounds within the framework. This indicates an approximately 4:1 ratio of MB^+ and TBA^+ in the frameworks.

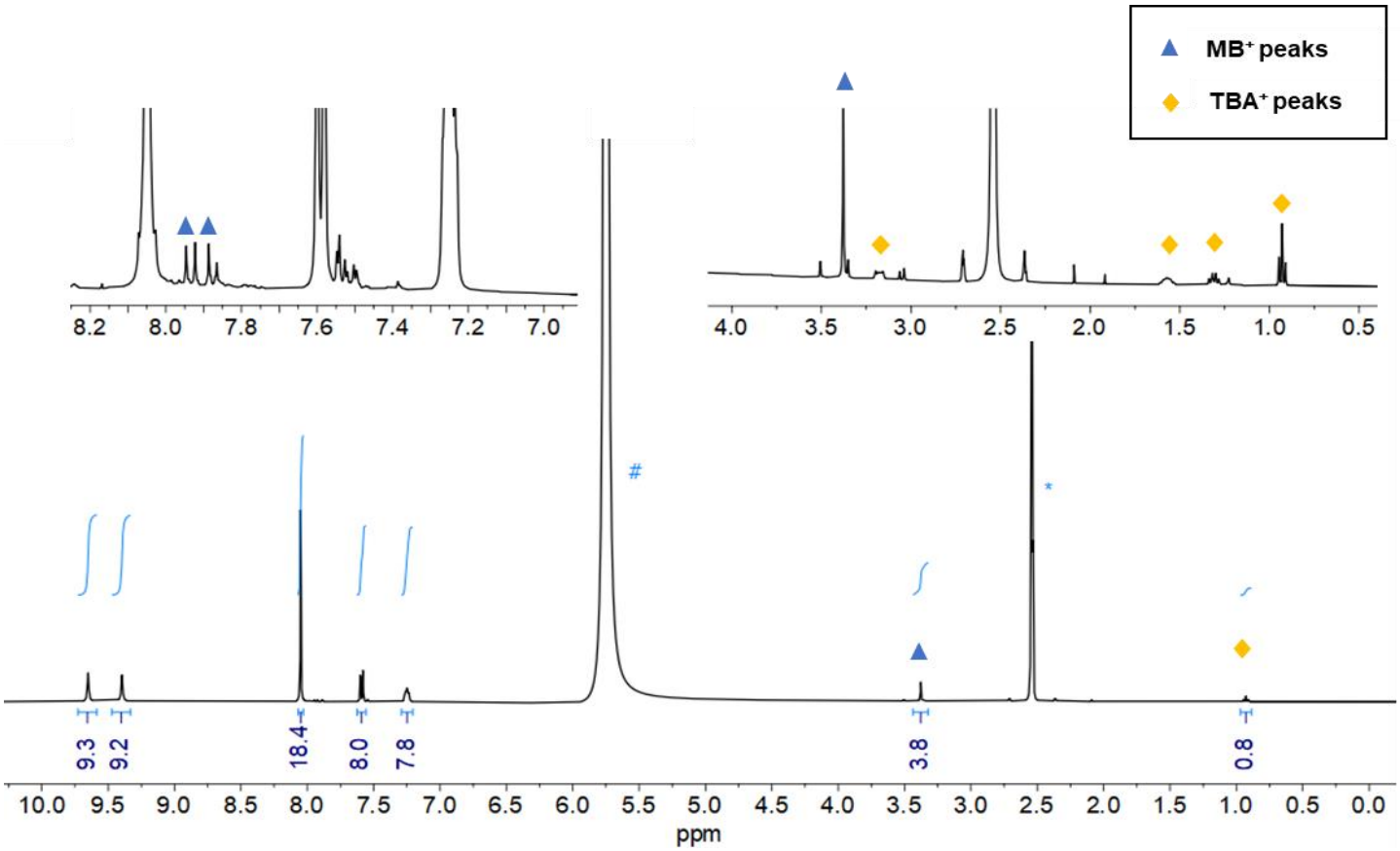

Figure S46. ^{1}H NMR spectrum of **TBA·2$_2$·B** after incubation with 28 µM $MB^+_{(aq)}$ solution for 14 days (d_6-DMSO containing a drop of $HCl_{(aq)}$).

References

1. H. E. Gottlieb, V. Kotlyar and A. Nudelman, NMR Chemical Shifts of Common Laboratory Solvents as Trace Impurities, *J. Org. Chem.*, **1997**, *62*, 7512-7515.

2. M. Morshedi, M. Thomas, A. Tarzia, C. J. Doonan and N. G. White, Supramolecular anion recognition in water: synthesis of hydrogen-bonded supramolecular frameworks, *Chem. Sci.*, **2017**, *8*, 3019-3025.

3. S. A. Boer, M. Morshedi, A. Tarzia, C. J. Doonan and N. G. White, Molecular tectonics: a node-and-linker building block approach to a family of hydrogen-bonded frameworks, *Chem. Eur. J.*, **2019**, *25*, 10006-10012.

4. P. Tomaszewski, M. Wiszniewski, J. Serwatowski, K. Woźniak, K. Durka and S. Luliński, Synthesis of tetraarylborates *via* tetralithio intermediates and the effect of polar functional groups and cations on their crystal structures, *Dalton Trans.*, **2018**, *47*, 16627-16637.

5. M. Solar and N. Trapp, *μ*CHILL: a lightweight, modular system for handling crystalline samples at low temperatures under inert conditions, *J. Appl. Crystallogr.*, **2018**, *51*, 541-548.

6. D. Aragão, J. Aishima, H. Cherukuvada, R. Clarken, M. Clift, N. P. Cowieson, D. J. Ericsson, C. L. Gee, S. Macedo, N. Mudie, S. Panjikar, J. R. Price, A. Riboldi-Tunnicliffe, R. Rostan, R. Williamson and T. T. Caradoc-Davies, MX2: A High-Flux Undulator Microfocus Beamline Serving Both the Chemical and Macromolecular Crystallography Communities at the Australian Synchrotron, *J Synchrotron. Radiat.*, **2018**, *25*, 885-891.

7. W. Kabsch, XDS, *Acta Crystallogr.*, **2010**, *D66*, 125-132.

8. *CryAlis Pro*, Oxford Diffraction, **2011**.

9. A. L. Spek, PLATON SQUEEZE: A Tool for the Calculation of the Disordered Solvent Contribution to the Calculated Structure Factors, *Acta Crystallogr.*, **2015**, *C71*, 9-18.

10. O. V. Dolomanov, L. J. Bourhis, R. J. Gildea, J. A. Howard and H. Puschmann, OLEX2: A Complete Structure Solution, Refinement and Analysis Program, *J. Appl. Crystallogr.*, **2009**, *42*, 339-341.

11. L. Palatinus and G. Chapuis, SUPERFLIP. A Computer Program for the Solution of Crystal Structures by Charge Flipping in Arbitrary Dimensions, *J. Appl. Crystallogr.*, **2007**, *40*, 786-790.

12. P. W. Betteridge, J. R. Carruthers, R. I. Cooper, K. Prout and D. J. Watkin, CRYSTALS Version 12: Software for Guided Crystal Structure Analysis, *J. Appl. Crystallogr.*, **2003**, *36*, 1487.

13. G. Sheldrick, SHELXT - Integrated Space-Group and Crystal-Structure Determination, *Acta Crystallogr.*, **2015**, *A71*, 3-8.